Biogeosciences Discussions

Biogeosciences Discussions is the access reviewed discussion forum of *Biogeosciences*

Short scale (6 h) temporal variation of sinking fluxes of planktonic and terrigeneous lipids at 200 m in the NW Mediterranean Sea

L. Méjanelle[1] and J. Dachs[2]

[1]LOOB – UMR CNRS 7651, Avenue Fontaulé, BP 44, 66650 Banyuls Sur Mer, France
[2]Department of Environmental Chemistry, IDAEA – CSIC, 18-24 C/Jordi Girona, 08034 Barcelona, Catalonia, Spain

Correspondence to: L. Méjanelle (laurence.mejanelle@obs-banyuls.fr)

Title Page

Abstract | Introduction

Conclusions | References

Tables | Figures

Back | Close

Full Screen / Esc

Printer-friendly Version

Interactive Discussion

Abstract

Drifting sediment trap measurements were carried out at high temporal frequency in the northwestern Mediterranean Sea in the course of the DYNAPROC2 campaign, during the transition between late summer to autumn conditions. Molecular biomarkers were

5   analyzed in selected subsets of consecutive samples collected for 6 h at 200 m depth. Fluxes of n-alkanes, long-chain alkenones, sterols and steroid ketones show high variability between consecutive 6-h samples, comparable in range to seasonal variability. n-Alkane export ranges from 1.4 to 29.7 μg m^{-2} d^{-1}, fluxes of C$_{37}$ alkenones varies from 0 to 14.2 μg m^{-2} d^{-1}. Fluxes of sterols, steroid ketones and C$_{30}$ alkane diol re-

10 spectively range from 31 to 377, 2.2 to 46 and 0.3 to 9.3 μg m^{-2} d^{-1}. Biomarker flux ranges are coherent with the relatively low primary production and the low export ratio encountered during the study. Molecular characteristics of biomarker composition is consistent with reworked algal and zooplanktonic organic matter with a remarkable refractory character. Lipid biomarker composition points to the dominance of haptophytes

15 over dinoflagellates in the exported material, and to a minor contribution of diatoms and eustigmatophytes. The intrusion of coastal water at the study site was recorded by an enhanced imprint of higher plant n-alkanes.

Two processes can be responsible for the pulses in biomarker flux: changes in the magnitude of particle flux (mass flux) and changes in the concentration of biomark-

20 ers in the particles. Most biomarkers show concurrent variability in fluxes. Pearson correlations between fluxes of biomarkers of haptophytes, dinoflagellates, eustigmatophytes, zooplankton activity and higher plants (alkenones, dinosterol, alkyl diols, dehydrocholesterol, steroid ketones) are significant ($p<0.01$, $n=31$). Biomarker fluxes are also significantly correlated to organic carbon flux. Concurrent variation of fluxes of

25 biomarkers suggest that the short term temporal variability of biomarker export fluxes depends primarily on the intensity of particle mass flux. Biomarker concentrations vary on a relatively narrower range than biomarker fluxes, indicating that changes in particle composition (due to degradation or source apportionment) has a weaker influence on

Short scale temporal variation of sinking fluxes

L. Méjanelle and J. Dachs

Printer-friendly Version

Interactive Discussion

flux variability. Thus, particle aggregation and sinking are key processes to explain the dynamic of biomarker export at a temporal scale of 6 h. Highest biomarker flux values recorded by the trap samples from 27 to 29 September correspond to highest values of zooplankton biomass integrated between the surface and 200 m. The decrease in
5 primary production after the October wind events is echoed by minima in biomarker flux values. Despite these correspondences, the coupling between primary production and biomarker export is complex.

1   Introduction

The fate of organic carbon produced by primary production is a central issue of the car-
10 bon cycle. Physical and biological forcing controls the carbon flow through ecosystem compartments and in the water column. The PECHE-DYNAPROC 2 program aims at better understanding these forcing in the Northwestern open Mediterranean Sea at the summer-fall transition when water stratification is disrupted by wind events. An interdisciplinary approach was set up to relate physical forcing, phytoplanktonic, zooplanktonic
15 and bacterial communities as well as related changes in inorganic and organic characteristics of dissolved and particulate phases, including sinking particles (Andersen et al., 2009).

The vertical export of biogenic particles results from biological production, aggregation, incorporation of ballast minerals, recycling in the surface ocean and vertical
20 sinking. The flux of organic compounds mirror the interplay of these processes. The molecular composition of lipid biomarkers of sinking particles reflects source organisms or contamination events, and informs on the freshness or degraded state of the organic matter (Matsueda and Handa, 1986; Wakeham and Lee, 1989; Wakeham and Beir, 1991; Burns et al., 2001, 2003; Christodoulou et al., 2009). Particles sinking in
25 the water column record temporal and spatial features of their generation and transformation in the upper ocean (Honjo, 1996). Time-course surveys have indeed showed that molecular biomarkers in sinking material recorded seasonal changes in the phy-

toplanktonic community, in particular at the study site (Marty et al., 1994; Wakeham et al., 2009; Sicre et al., 1999). Many biological processes show short-term variability, in particular day-night changes. However, to which degree this variability is transferred to the export of organic matter remains largely unknown. A previous work at the DYFAMED site during spring showed that lipid export variability over timescale of 4 h was in the same range as seasonal variability (Goutx et al., 2000). Another study in a frontal system of the Alboran Sea showed differences between day and night fluxes of biomarkers less 50% (Tolosa et al., 2005). The present contribution assesses the molecular composition of sinking particles collected at 200 m by drifting sediment traps using a sampling frequency of 6 h. Vertical fluxes of aliphatic and steroidal alcohols, long-chain alkenones and hydrocarbons are determined.

Environmental parameters and ecological information determined in the frame of the DYNAPROC 2 program helps deciphering the sources of phytoplanktonic biomarkers and tackling drivers of temporal variability of flux high frequency variability.

2   Material and methods

2.1   Cruise track and sample collection

The DYNAPROC2 cruise took place between 13 September and 17 October 2004 in the Northwestern Mediteranean Sea, 28 miles offshore from Nice (France) (Andersen et al., 2009). The sampling zone was a grid of 16 stations defined by the crosses in Fig. 1, at the vicinity of the French JGOFS Station DYFAMED (43°25′ N, 7°52′ E). Sinking particles were collected using Technicap PPS5 sediment traps (1 m² collecting area) drifting at 200 m depth. Traps were allowed to drift in this area while other sampling operations took place. When traps occasionally drifted out of this zone, they were retrieved and replaced at the original site. Carousels of 24 collecting cups were programmed with a 6 h-time resolution. Four series of samples were collected: the A series from the 17 to the 22 September, the B series from the 23 to 29 September, the

C series from the 3 to the 8 October and the D series from the 10 to the 15 October (Table 1). Before mooring, collecting cups were poisoned by a 2% buffered formalin solution made with filtered seawater. Upon trap recovery, swimmers were removed and the collected material was split using a wet suspension divider. One tenth of the samples was dedicated to this study and kept frozen until analysis. The other fractions were dedicated to bulk analyses (2/10th), pigment (2/10th) and lipid class analyses (1/10th) and the results are reported and discussed in detail by Marty et al. (2009). Four other fractions were dedicated to mass flux and colored matter analyses, but these results could not be successfully acquired due to the low levels of material available. The accuracy of sample splitting is demonstrated by the reproducible trends in sterols fluxes measured by two distinct methods on one tenth of the sample, by Iatroscan (Marty et al., 2009) and by GC/FID (Fig. S1, Supplementary material at http://www.biogeosciences-discuss.net/6/7673/2009/bgd-6-7673-2009-supplement.pdf).

2.2 Lipid extraction, separation, and analysis

The supernatant of sediment trap samples were shown to contain lipidic compounds accounting for 15 to 75% of the total trap material when the collection time was in the order of weeks to one month (Körtzinger et al., 1994). In colder waters, the dissolution of fatty acids into the dissolved supernatant of the trap collecting cups still accounted for half of the flux (Budge and Parrish, 1998). Beside organics, about 30% of inorganic phosphorus was also reported to occur in sediment trap supernatant (O'Neill et al., 2005). A challenge of the present study was the small sample size: one tenth of 6 h-collection of sinking particles in a low productivity area. To maximize the recovery of lipids from the trap material, the extraction procedure was set to recover the lipids from the particles and from the supernatant of the trap, as well as lipids that may leach during freezing and thawing. After thawing, the samples were centrifuged and the water phase was extracted by liquid liquid extraction using CH_2Cl_2. The obtained solution was used to extract the particles according to a modified Bligh and Dyer (1959) method where CH_2Cl_2 replaced CH_3Cl_3. Known amounts of surrogates were added

Title Page

Abstract | Introduction

Conclusions | References

Tables | Figures

◀ | ▶

◀ | ▶

Back | Close

Full Screen / Esc

Printer-friendly Version

Interactive Discussion

Short scale temporal variation of sinking fluxes

L. Méjanelle and J. Dachs

Title Page

Abstract | Introduction

Conclusions | References

Tables | Figures

⏮ | ⏭

◀ | ▶

Back | Close

Full Screen / Esc

Printer-friendly Version

Interactive Discussion

to the samples prior extraction: $C_{24}D_{50}$, C_{21}-OH and androstanol were used as surrogates for hydrocarbons, alkanols and sterols, respectively. Particles were extracted by 15 min of contact in a CH_2Cl_2-H_2O-CH_3OH solution (1/0.8/2; v/v/v) and the liquid phase was pipetted out after 5 min of centrifugation. Two other extractions were carried out by sonication for 15 min in the solvent mixture and all the liquid phases were combined into a decantation flask. After adding H_2O and CH_2Cl_2 to reach the proportions where two phases appear, the phases were shaken and allowed to decant for 30 min. The organic phase was collected, and the aqueous phase was rinsed twice with 20 ml of CH_2Cl_2. All combined organic extracts were dried overnight over $MgSO_4$, filtered and reduced by rota-evaporation. Total lipids were separated into various lipid classes using SEP-PACK Si-NH2 glass cartridges purchased from Macherey Nagel. The method was adapted from Hinrichs et al. (2000) and the recovery of the selected lipid classes was validated using standards ($C_{24}D_{50}$ $C_{36}H_{74}$ and squalene for hydrocarbons; a previously analyzed fraction of long chain alkenones for ketones; C_{21}-OH, androstanol, coprostanol, cholesterol and lanosterol for alcohols; the quantities were in the upper range of those occurring in the samples). The cartridge was conditioned by 10 ml of hexane and the sample was spotted on its top in 150 μl of heptane. The first fraction was eluted by another 3.850 ml of hexane and contained the hydrocarbons. The second fraction, comprising long-chain alkenones was eluted by 6 ml of hexane/CH_2Cl_2 (3:1, v/v). The third fraction was eluted by 5 ml CH_2Cl_2/aceton (9:1, v/v) and contained n-alkanols, sterols, n-alkyl diols and hydroxy-ketones. The fractions were reduced by rota-evaporation and transferred to vials for gas chromatography analysis.

The hydrocarbons were analyzed using a Hewlett-Packard HP5890 gas chromatograph (GC) and a JW DB5 (Chrompack) column (50 m, 0.32 mm internal diameter, 0.25 μm film thickness). The oven temperature was programmed to rise from 60°C to 100°C at 25°C min^{-1}, then to 310°C at 2°C min^{-1} (80 min hold time). The injector was an on-column injector programmed on the oven track mode, the detector temperature was 330°C and the carrier gas was Helium set at a pressure of 1.1 bar.

Long-chain ketones were analyzed using a non-polar column (CP Sil 5 CP, 50 m,

0.32 mm internal diameter, 0.25 μm film thickness) and a Hewlett-Packard HP5890 chromatograph, with the oven temperature rising from 80°C to 140°C at 30°C min^{-1}, then to 280°C at 15° min^{-1}/and to 310° at 0.5° min^{-1}, followed by a temperature hold of 60 min. The GC was equipped with an on-column injector programmed to track the oven temperature and a FID detector at 320°C and helium was used as carrier gas at a pressure of 0.98 bar. Prior to analyses, a known amount of $C_{36}H_{74}$ was added as injection standard to the fractions.

Alcohols were transformed into the corresponding trimethylsilyl ether derivatives (TMS) using a mixture of bis(trimethylsilyl)-trifluoroacetamide and trimethylchlorosilane (99:1, Silyl-99) purchased from Macherey-Nagel (Germany) and pyridine during 60 min at 80°C. TMS of alcohols were analyzed on a non-polar column (JW DB5, 30 m, 0.32 mm internal diameter, 0.25 μm film thickness) and an Agilent 6890N chromatograph, using the following oven temperature program: 60° (1 min)/25° min^{-1}/100°/15° min^{-1}/150°/3° min^{-1}/300° (>60 min). The GC was equipped with an on-column injector programmed to track the oven temperature and a FID detector at 320°C and helium was used as carrier gas at a pressure of 0.8 bar.

GC coupled to mass spectrometry (MS) and co-injection with authentic compounds of known structures confirmed the identities of the major components. GC/MS analysis of lipids was performed on an Agilent 6890 GC coupled to an Agilent 5973 quadrupole mass spectrometer. The GC was equipped with an on-column injector programmed on the oven track mode, a JW DB5-MS column (0.25 mm internal diameter, 0.25 μm film thickness) and the carrier gas was helium with a flow of 1.2 ml min^{-1}. The interface temperature was 280°C. MS operating conditions were: ion source temperature of 230°C, quadrupole temperature 150°C, electron impact energy of 70 eV, the scanned mass range was 40–600 atomic mass units at 0.6 scan s^{-1}. The chromatographic columns used were DB5 with oven programs as previously described.

The quantification of hydrocarbons and sterols was carried out using the surrogates used as internal standards. Long-chain ketones were quantified using the injection standard.

Title Page

Abstract | Introduction

Conclusions | References

Tables | Figures

|◄ | ►|

◄ | ►

Back | Close

Full Screen / Esc

Printer-friendly Version

Interactive Discussion

The formalin solution used to poison the traps was analyzed using the same procedure as the samples to estimate whether it contributed targeted compounds to crude extracts of samples.

2.3 Hydrocarbon and sterol nomenclature

The nomenclature used to design hydrocarbons is C_x for saturated aliphatic homologues, where x is the number of carbon of the aliphatic chain, and $C_{x:y}$ for unsaturated hydrocarbons, y being the number of double bonds. *n*-Alkanols are designed C_{x-OH}, x is the number of carbon of the aliphatic chain. The nomenclature used to design sterols is used for the graphics only and is detailed in the first figure's legend where they appear.

The carbon preference index (CPI) of *n*-alkanes is calculated as:

$$CPI_{24-34} = \frac{1}{2} \times \left(\frac{(C_{25} + C_{27} + C_{29} + C_{31} + C_{33})}{(C_{24} + C_{26} + C_{28} + C_{30} + C_{32})} + \frac{(C_{25} + C_{27} + C_{29} + C_{31} + C_{33})}{(C_{26} + C_{28} + C_{30} + C_{32} + C_{34})} \right).$$

2.4 Statistical analyses

Pearson correlations between data were computed using SPSS[®] Software version 17.0.

3 Results

Five groups of consecutive samples were selected for the present study on the basis of visual examination of the samples. The first part of the A series (17 and 18 September) and the samples from the D series (12 and 13 October) showed few visible particles whereas particles could easily be observed in the other groups of consecutive samples from the A, B and C series.

3.1 Physical and biological environment

Characteristic hydrological and meteorological conditions of the cruise are detailed in Andersen et al. (2009). Briefly, the hydrological conditions are typical of late summer situation with a stratified water column and the location of the thermocline at 25 m depth, with surface temperatures above 20°C (up to 22°C during calm periods). The meteorological regime is characterized by the alternation of strong wind events and calm periods. Two NE wind events occur during the collection of trap series A and B (Fig. 2) and it rained significantly before the start of the cruise and during the wind events. An intrusion of low salinity (<38.3 PSU) coastal water is evidenced between 15 and 75 m depth while the water column remains stratified (Fig. 2, top pannel; Andersen et al., 2009). Intrusion of coastal water shows that the central part of the Ligurian Sea is susceptible to receive local lateral advection (Stewart et al., 2007). A succession of wind events from SW, NE and SW directions occurs between the 11 and the 16 October, at the end of the collection of the trap series C and D (series sampled from the 3 to the 15 October). The thermocline deepens to 40 m depth and the mixed layer cools down to 16°C. This destratification suggests that the transition from late summer to autumnal condition is initiated at the end of the cruise. A second intrusion of low salinity water is recorded at the study site between the 9 and 11 October, less in intensity than the previous similar event (Fig. 2).

Pigments analyses showed that phytoplankton is dominated by pico- and nano-autotrophs (around 87%, Marty et al., 2008). Microphytoplankton is dominated by dinoflagellates while senescent diatoms are present at subsurface at the beginning of the cruise and around the 5 October (Marty et al., 2008; Lasternas et al., 2008). Primary production varies between 97 and 310 mg C m^{-2} 12 h^{-1}, which is consistent with the oligotrophic character of the area in late summer (Marty et al., 2009). Integrated chlorophyll-*a* however showed higher values (20 to 40 mg m^{-2}) than those typical of this time of the year at the beginning of the cruise, in association with the occurrence of senescent diatoms at subsurface (Marty et al., 2008). Zooplankton was dominated

Title Page

Abstract | Introduction

Conclusions | References

Tables | Figures

◀ | ▶

◀ | ▶

Back | Close

Full Screen / Esc

Printer-friendly Version

Interactive Discussion

by copepods from the 17 to the 30 September, whereas their contribution slightly decreased in October in favor of other predators like Pteropods and other carnivorous predators (Mousseau et al., 2009; Raybaud et al., 2009).

3.2 Hydrocarbons

The formalin solution used to preserve the samples contributed some dissolved hydrocarbons in negligible quantities except for C_{19} and C_{23} n-alkanes; therefore both alkanes are not reported here. Hydrocarbon composition is reported in Table 2. They encompass n-alkanes in the C_{12}–C_{37} range with an even predominance from C_{12} to C_{26} and an odd predominance for the C_{27}–C_{36} homologues. The even predominance of low molecular weight n-alkanes is an unusual profile, reported in other few situations. For instance, C_{16}, C_{18} and C_{20} also dominated hydrocarbons in sinking particles from the Western Mediterranean Sea and from the Laurentian Great Lakes (Dachs et al., 1998; Parrish et al., 1992). Odd alkanes also characterized sediment trap material collected in the Mediterranean Sea, together with a high abundance of methylalkanes and diploptene, and were associated to the contribution of cyanobacteria (Dachs et al., 1998). The occurrence of alkanes with even carbon number has also been related to bacterial reworking of organic matter (Grimalt and Albaigés, 1988). In the present report, diplotene is a minor compound and methylalkanes could not be detected. Other hydrocarbons detected in the samples have an algal origin: C_{15}, C_{17} (Clark and Blumer, 1967), pristane, lycopane (Sinninghe Damsté et al., 1993) as well as $C_{37:2}$ and $C_{37:3}$ synthesized by alkenone-producing haptophytes (Volkman et al., 1980). These phytoplanktonic biomarkers occur in low percentages (Table 2). At the same study site, a high flux event was recorded at 200 m in April 1987 and C_{17} was the dominant n-alkanes (20%, Marty et al., 1994). In comparison, C_{17} abundances measured in the present time series samples are lower (0.8 to 5.2% of hydrocarbons, Table 2) which indicates that fresh phytoplanktonic inputs did not dominate the sinking material or that there was an efficient degradation of low MW alkanes during sinking. The relative contribution of C_{17} to n-alkanes peaks at the beginning of the D series, on

Short scale temporal variation of sinking fluxes

L. Méjanelle and J. Dachs

the night of the 12 to the 13 October, while the D series corresponds to weak fluxes. Odd-chain alkenes in the C_{15}–C_{19} range and $C_{21:6}$ are phytoplanktonic biomarkers commonly found in sinking particles rich in fresh phytoplanktonic residues (Burns et al., 2003) and they are rapidly degraded during particle decay (Matsueda and Handa,
5   1986). None of these indicators for fresh algal residue could be detected in sinking particles collected during DYNAPROC 2 cruise.

No unresolved hydrocarbon mixture, sourced by petroleum contamination, could be evidenced, nor hopanes nor steranes; however the detection of the humps and of petroleum biomarkers on the chromatograms may have been impeded by the low quan-
10 tities of material analyzed.

A moderate odd-to-even carbon number predominance or an even preference characterizes C_{24} to C_{34} n-alkanes in samples where long-chain n-alkanes fluxes showed lowest contribution (Fig. 2). In contrast, the samples with a clear odd predominance of long-chain n-alkanes correspond to maxima in C_{25}–C_{37} odd n-alkanes fluxes
15 ($>2\,\mu g\,m^{-2}\,d^{-1}$). This signature is characteristic of terrestrial higher plants (Eglinton and Hamilton, 1967) whereas lower CPI values point to petroleum or marine organism inputs (Davis, 1968; Han and Calvin, 1969; Cripps, 1990).

The hydrocarbons which relative abundances show greater variations are squalene, squalane and long-chain n-alkanes. Squalene is likely contributed by zooplankton
20 (Wakeham and Canuel, 1986, 1988). Its observed variation trend is quite erratic with increases and decreases up to 5 folds in consecutives 6 h-samples. Moreover, maxima occurred during the day as well as at night. Total hydrocarbon fluxes describe ample variations between 1.4 and $29.7\,\mu g\,m^{-2}\,d^{-1}$ without clear day-night periodicity (Table 2, Fig. 3).

25 **3.3 Long-chain alkenones**

C37 and C38 unsaturated methyl and ethyl alkenones are synthesized by a few haptophytes, in particular the worldwide distributed coccolithophorids *Emiliania huxleyi* and *Gephyrocapsa oceanica* (Conte et al., 1992). They are unequivocal biomarkers for

Short scale temporal variation of sinking fluxes

L. Méjanelle and J. Dachs

haptophytes. They could be detected in most of the samples except for the D series (Table 3). The alkenone unsaturation index UK'_{37}, defined as $UK'_{37} = \frac{37:2}{37:2+37:3}$, is related to the growth temperature of the algae and is used to reconstruct sea surface temperatures (SST) from UK'_{37} measured in old sediments (Prahl et al., 1988). SST estimates may be overestimated when the chromatographic peak of the methylalkenone $C_{37:3}$ is not well above the noise or when the capillary column has been used for a while (Villanueva and Grimalt, 1996; Grimalt et al., 2001). For instance, we considered that a peak area of methylalkenone $C_{37:3}$ above 2500 mV s enables a proper determination of UK'_{37}. Two samples at the start of the A series and one at end of the D series, with lower peak areas, were discarded for the calculation of UK'_{37}. SST estimates reconstructed using the Prahl et al. (1988)'s calibration varied between 13 and 21°C (Fig. 3). Reconstructed temperature estimates are in the range of the CTD hydrocast temperatures from 20 to 30 m for the A and B series-samples. They are higher for the C and D series samples and correspond to hydrocast temperature above 20 m. The sample from the D series is collected after the mixing of the water column and alkenone composition may have adapted to the changing temperature. When the C series is collected, the water is still well stratified and the results rather suggest that haptophytes producing alkenones are situated slightly higher in the water column. The depth of production of alkenones is in good agreement with that inferred from alkenones in suspended particles in November, whereas the depth of production of alkenones during spring and early summer is deeper (Ternois et al., 1997).

Fluxes of alkenone and alkenoates range from to 1.0 to 33.8 $\mu g\,m^{-2}\,d^{-1}$, and C37 alkenone fluxes 0.4 to 14.28 $\mu g\,m^{-2}\,d^{-1}$, with increases or decreases up to ten fold between consecutive 6 h-samples (Table 3 and Fig. 3). Alkenones and C37:3 and C38:3 homologous long-chain alkenes show synchronous maxima in fluxes (Fig. S2 Supplementary material). The ratio of alkenones to homologous alkenes varies over one order of magnitude (Fig. S2 Supplementary material, http://www.biogeosciences-discuss. net/6/7673/2009/bgd-6-7673-2009-supplement.pdf). The geochemical significance of this ratio is unknown at present. If long-chain alkenes are intermediates of the biosyn-

Short scale temporal variation of sinking fluxes

L. Méjanelle and J. Dachs

Title Page

Abstract | Introduction

Conclusions | References

Tables | Figures

|◄ | ►|

◄ | ►

Back | Close

Full Screen / Esc

Printer-friendly Version

Interactive Discussion

thesis or the catabolism of alkenones, this ratio may be related to the physiological state of alkenone producers.

3.4 Alkanols, sterols and steroidal ketones

Alcohols constitute the most abundant of the targeted lipid classes with fluxes one order of magnitude above those of hydrocarbons and of long-chain alkenones. The alcohol fraction is dominated by 24-methylcholesta-5-dien-3β-ol (brassicasterol) and cholest-5-en-3β-ol (cholesterol) (Fig. S3, Supplementary material). Four other sterols have abundances above 5%: 27-nor-24 methylcholesta-5,22E-dien-3β-ol, cholesta-5,22E-dien-3β-ol, 24-ethylcholesta-5,22E-dien-3β-ol and 24-ethylcholestan-5-en-3β-ol (Table 4, Fig. S3 Supplementary material). This composition resembles that determined in sediment traps from the same site between March and June 2003, however with a noticeably higher contribution of 24-methylcholesta-5,22E-dien-3β-ol (Wakeham et al., 2009).

4-Methylsterols having additional methyl groups substituted at C23 or both at C23 and C24 were identified in the sinking particles, with 4α,23,24-trimethylcholest-22-en-3β-ol (dinosterol) as the major homologue (2.5±0.5% of total sterols, Fig. S3 Supplementary material). Other sterols stemming from dinoflagellates are identified in the sinking particles. 23,24-Dimethylcholesta-5,22E-dien-3β-ol and its stanol counterpart contribute from 2.1 to 3.8% of total sterols, and 4α,24-dimethylcholestan-3β-ol occurs at trace levels.

C26 Sterols having 27-nor or 24-nor structures accounted for a non negligible part (6.5 to 12.5%, Fig. S3 of Supplementary material) of total sterols, with 27-nor-24-methylcholesta-5,22E-dien-3β-ol ranking in the five more abundant sterols (4.7 to 8.7% of total sterols).

24-Methylcholesta-5,24(28)-dien-3β-ol, often used to fingerprint diatom occurrence, accounts for a few percent of total sterols (Fig. S3). C29 sterol with Δ5,24(28) double bond system is also identified in all trap samples in small amounts and is synthesized by Prasinophyceae, dinoflagellates and diatoms. Two isomers of 24-propylcholesta-

Short scale temporal variation of sinking fluxes

L. Méjanelle and J. Dachs

Title Page

Abstract | Introduction

Conclusions | References

Tables | Figures

◀ | ▶

◀ | ▶

Back | Close

Full Screen / Esc

Printer-friendly Version

Interactive Discussion

5,24(28)-dien-3β-ol are identified in the sinking particles and have been previously reported in Mediterranean samples, including in sediment trap from the study site (Tolosa et al., 2003; Christodoulou et al., 2009). Its biological precursor is yet unknown.

A series of steroid ketones was identified in the samples (Table 4). 24-norcholesta-4,22E-dienone, cholestanone and cholest-4-en-3-one were chromatographically resolved from sterols whereas another isomer of cholestanone coeluted with 5α(H)-cholestan-3β-ol, and cholestadienone occurred in a composite peak with 4-methylcholesta-24(25)-en-3β-ol in some samples. Other homologues with mass peak of 412 and 414 daltons eluted at the end of the elution time span of sterols. However, their poor peak shape and the mismatch between their retention time under GC and GC-MS conditions (constant gas pressure fit versus constant gas flow) made their quantification and their attribution tricky; therefore they were not further considered. Cholest-4-en-3-one was the dominant steroidal ketone and accounted for up to 19.5% of the compounds in the alcohol fraction, alike in sinking particles from various location (Wakeham and Canuel, 1986). The timing of its flux shares some similarities with that of sterols, with no obvious maxima at night (Fig. 6).

C30 mid-chain alkane diols and C30 hydroxy mid-chain alkanone were detected in comparable amounts (Table 4). Eustigmatophytes are generally considered as the source of mid-chain hydroxy alkanols in marine sediments (Volkman et al., 1992, 1999; Gelin et al., 1997; Versteegh et al., 2000).

High-molecular weight n-alkanols are indicative of terrigeneous higher plants and are little abundant in the present series of samples. Their flux pattern shows synchronous characteristics with that of long-chain n-alkanes, and linear correlation between both biomarker groups explains 67% of their variability (Fig. 2). Long-chain n-alkane abundances accounted for two to four folds those of long-chain n-alkanols except for the last series of samples where they reached 12 times long-chain$n$-alkanol abundances.

Total sterol fluxes ranged from 31 to 377 μg m^{-2} d^{-1} and their timing is similar to that of long chain alkenones (Fig. 3).

4 Discussion

4.1 Occurrence of lipidic biomarkers and nature of exported particles

The analysis of molecular biomarkers in one tenth of sediment trap material collected during 6 h in an oligotrophic area represented a challenge because of the low amounts of material. Hydrocarbons and sterols could be quantified in all studied samples, while alkenones could not be detected or inappropriately quantified in a few samples.

Steroid ketones occur in minor abundances are in marine organisms and are produced by microbial oxidation of sterol, for instance cholest-4-en-3-one is produced by degradation of cholest-5-en-3β-ol (Wakeham and Canuel, 1986, 1988; Burns et al., 2003). Their relative abundance in sediment trap tend to increase with depth (Wakeham and Lee, 1989; Burns et al., 2003). The ratio of cholest-4-en-3-one to cholest-5-en-3β-ol in the sinking particles collected during DYNAPROC 2 is in the upper range or higher than values measured in sediment traps at the same site during spring bloom and post-bloom conditions (May–June, Christodoulou et al., 2009), suggesting a more intense reworking in the late summer conditions. Pigments of sinking particles are characterized by the dominance of phaeopigments over intact chlorophylls, which also denotes that phytoplanktonic remains are degraded (Marty et al., 2009). The concurrent variation in fluxes of phaeopigments and molecular biomarkers suggests a common vector of transport, fecal pellets (Fig. S4 Supplementary material, http://www.biogeosciences-discuss.net/6/7673/2009/bgd-6-7673-2009-supplement.pdf).

24-Ethylsterols are synthesized by higher plants and are possibly related to fluvial and aerosol inputs. No major rivers are located in the vicinity of the study site and the area of study is located in the central Ligurian Sea, where the Ligurian current prevents inputs of coastal waters (Béthoux and Prieur, 1983). However, advective inputs occasionally occur (Steward, 2007), as evidenced by the intrusion of low salinity coastal waters during DYNAPROC 2 (Andersen et al., 2009). After the intrusion of coastal waters, a stronger higher plant imprint in *n*-alkanes indicates the incorporation of terrigeneous material to the rain of particles, whilst no increase in C$_{29}$ sterol

abundances was recorded. Aerosols inputs are significant at the study site (Migon et al., 2001; Guieu et al., 2002) and constitute a potential source of C_{29} sterols. The ratio of terrigeneous alkanols, cholest-5-en-3β-ol, 24-ethylcholest-5-en-3β-ol and 24-ethylcholest-5,22E-dien-3β-ol to terrigeneous alkanes in marine aerosols are reported in Table 5. In marine aerosols, the ratio of 24-ethylcholest-5-en-3β-ol to terrigeneous long-chain n-alkanes takes values varying from 0.01 to 0.81, whereas the values are one order of magnitude higher in sinking particles (5.6±3.5%). Similar behavior is observed for cholest-5-en-3β-ol and 24-ethylcholest-5,22E-dien-3β-ol. Consequently, aerosol inputs accounts only for a small portion of C29 sterols and algae likely constitute their dominant source.

4.2 Relationships between lipidic biomarker composition and phytoplanktonic community

During DYNAPROC 2, primary productidivity was measured, specific abundances of microphytoplankton was determined by microscopy and pigment analyses gave a complementary view of the whole phytoplanktonic community (Lasternas et al., 2008; Marty et al., 2008). Pigment chemometry indicated that the phytoplankton is dominated by small forms (haptophytes="prymnesiophytes", pelagophytes, prasinophytes, cyanobacteria and prochlorophytes) whereas diatoms and dinoflagellates contributed to 3 to 18% of chlorophyll-a (Marty et al., 2008). This characteristic is in agreement with the oligotrophic character of the system at this time of the year. The good description of the phytoplanktonic community present in the water column set a pertinent framework to attempt to decipher the biological sources of sterols exported by sinking particles in a oligotrophic Mediterranean oligotrophic system.

24-Methylcholesta-5,22E-dien-3β-ol (brassicasterol) is almost the exclusive sterol of haptophytes, a major component of the plankton in the water column (Marty et al., 2008). This sterol often accounts for more than 90% of sterols in some diatoms species from productive area (*Chaetoceros simplex*, *Skeletonema costatum*, *Thalassiosira pseudonana*, *Nitzschia alba*) which are not detected in the plankton of the water

column (Lasternas et al., 2008). In addition the pigment signature of diatoms is almost absent in the exported particles (Marty et al., 2009). A diatom contribution to the source of brassicasterol thus can be discarded. Brassicasterol represents 53% of total sterols in the dinoflagellates *Gymnodinium simplex* (Conte et al., 1994; Volkman, 1986), while *Gymnodinium* is one of the dominant genus of dinoflagellates at the time of study (Lasternas et al., 2008).

24-Ethylcholest-5-en-3β-ol (sitosterol) is an important component of dinoflagellates and haptophytes, of a few Prymnesiophycea and Raphidophytes (Volkman, 1986; Nichols et al., 1987; Volkman et al., 1993). Its occurrence in diatoms is not relevant here, as it concerns genera insignificant in the water column (*Asterionella* and *Navicula*, Lasternas et al., 2008). In DYNAPROC 2 sinking particles, the proportion of sitosterol to alkyl diols denies that eustigmatophytes are a foremost source for this sterol (Volkman et al., 1992; Méjanelle et al., 2003). In this context, sitosterol is likely sourced by Haptophytes and dinoflagellates, both significant algal groups in the water column. The high abundance of haptophytes could account for the dominance of 24-methylcholesta-5,22E-dien-3β-ol and for the relative high abundance of 24ethylcholest-5-en-3β-ol in sinking particles.

The other dominant C29 sterol in sinking particles is 24-ethylcholesta-5,22E-dien-3β-ol. It is reported in significant amounts in algae that are little significant during this study according to pigment chemometry (Cryptophycea and Chlorophyceae, Marty et al., 2008). It is also a component of Rhodophyceae and Chrysophyceae whose occurrence during DYNAPROC 2 study is not known (Volkman, 1986; Dunstan et al., 2005). The sterol compositions of pelagophytes and prochlorophytes, two dominant groups in the oligotrophic situation encountered during this work, are unknown at present. Whether these algae may contribute to the remarkable abundance of C29 sterols remains an open question. The gap of knowledge concerning sterols of pico and nanophytoplanktonic species of oligotrophic situations is a drawback for deciphering the information brought by sterols. Improving our knowledge on sterols of nano and picoplankton would be a benefit for paleooceanographic studies addressing the Mediter-

ranean Sea and other oligotrophic environments.

The high abundances of cholest-5-en-3β-ol (cholesterol) and the cholesta-5,22E-dien-3β-ol (dehydrocholesterol) in the DYNAPROC 2 sinking particles suggest an important zooplanktonic contribution. High proportions of cholesterol are have also been
5 reported in some dinoflagellates such as the *Gonyaulax* genus, which is not an important phytoplanktonic component at the time of this study (Lasternas et al., 2009), in haptophytes and in some diatoms (Volkman, 1986). Sterols in cultures of cyanobacteria were dominated by a mixture of cholesterol and sitosterol (Volkman, 1986), but further examination proved cyanobacteria to be devoid of sterols (Summons et al., 2006).
10 Therefore, the occurrence of cholesterol in sinking particles is related to zooplankton and remains of haptophytes.

Haptophyte are specific producers of alkenones. A pluriannual study of alkenone export at the study site and the same depth showed maxima at the end of the spring bloom (April to June) and in October–November with considerable interannual dif-
15 ferences in flux maxima (Sicre et al., 1999; Ternois et al., 1996). The maxima in fluxes measured during DYNAPROC 2 are comparable maxima measured in 1989, and higher than maxima measured in 1993 and 1994 (Sicre et al., 1999).The average flux of C37 alkenones measured during this study ($3.1 \pm 3.7 \, \mu g \, m^{-2} \, d^{-1}$) is lower than the flux maxima of 1989, but still higher than flux maxima of 1993 and 1994. Even-
20 though the fall disruption of the upper thermocline was only initiated at the end of the cruise, the fall bloom of alkenone producers may be occurring or starting.

The low abundance of dinosterol and dinostanol reflect the small contribution of microphytoplankton to the whole autotrophs, eventhough dinoflagellates represent the dominant group of microphytoplankton (Marty et al., 2008; Lasternas et al., 2008,
25 Fig. 4). Dinosterol and dinostanol are abundant sterols of dinoflagellates, in particular in *Gymnodinium* which stands as one of the dominant dinoflagellate genus during this study (Volkman, 1986; Piretti et al., 1997; Mansour et al., 2003; Lasternas et al., 2008). The other sterols substituted at C4 more likely fingerprint the remains of dinoflagellate in the sinking particles. 4α,24-Dimethyl substitued sterols are identified

in variable amounts in *Scripssiella* and *Gymnodinium* (Harvey et al., 1987; Mansour et al., 2003), relatively abundant in the microplankton and thus susceptible of having contributed these sterols. Dinoflagellate genus comprising sterols substituted at C23 and C24 in the literature do not correspond to significant genera in the water column (Lasternas et al., 2008). C26 sterols are not systematically reported in studies dealing with sterols. However they are reported in marine dinoflagellates, in particular in the genus *Gymnodinium* (Goad and Whithers, 1982; Volkman, 1986), that dominates the dinoflagellates during the present study (Lasternas et al., 2008) and a possible source of these sterols.

4.3 Timing and drivers of biomarker flux variation

Little is known about particle export at high resolution time scale. A previous study showed important variability of export fluxes of proteins and lipid classes with a 4-h time resolution at the same site during the spring transition (Goutx et al., 2000). In the frontal structure of the Alboran Sea, no substantial variation in sterol and alkenone fluxes was observed between day and night (<50% night-time change), indicating that the export flux resulted mainly from passive sedimentation of phytoplanktonic material (Tolosa et al., 2005). The present study confirms a high variability of biomarker sedimentation at 6 h time resolution, characterized by pulses in fluxes up to 6-folds. For non aromatic hydrocarbons and alkenones, the range of the variability with a temporal resolution of 6 h is of the same magnitude of seasonal variability at the same site (Ternois et al., 1997; Marty et al., 1994). Sterols decay during particle sinking complicate the comparison with other worldwide situations because the literature on sterol fluxes concern sediment traps mostly moored at deeper depths (Table 5). Sterol fluxes measured during DYNAPROC2 compare well to those measured in High Nutrient Low Chlorophyll Antarctic site at the same depth (Table 5), which characterizes a weak export. This is in good agreement with low bulk parameter export fluxes measured during DYNAPROC 2 and with the relatively low primary production (Andersen et al., 2009; Marty et al., 2009).

Short scale temporal variation of sinking fluxes

L. Méjanelle and J. Dachs

Title Page

Abstract | Introduction

Conclusions | References

Tables | Figures

◀ | ▶

◀ | ▶

Back | Close

Full Screen / Esc

Printer-friendly Version

Interactive Discussion

During the present study, the microphytoplankton and the nano and picoplankton show clear changes at the time scale of a few days (Marty et al., 2008; Lasternas et al., 2008). Phytosterol composition of the exported material is rather constant over time and failed to reflect this evolution (Fig. 5). Linear correlations between fluxes of biomarkers stemming from haptophytes, dinoflagellates, alkenone producing- haptophytes and eustigmatophytes explain 74 to 97% of their variance, further supporting a synchronous export of remains issued from distinct groups of phytoplankton (Table 7). The low export ratio and consequent high residence time of organic matter likely results in a temporal integration of biomarker signature in the exported particles over a larger period than the sampling frequency. This integration, in addition to aggregation-dissagregation processes may have blurred the variability of phytoplanktonic sources existing in the water column.

Chlorophyll-*a* integrated over the water column showed a diel variation during DYNAPROC 2 cruise (Marty et al., 2008), and the exported organic matter (POC) flux echoed this variation (Marty et al., 2009). Maxima in export of some lipid classes were also observed at night at the end of spring (Goutx et al., 2000). However, for the subset of 31 samples under consideration here POC fluxes failed to show an obvious day-night periodicity (Fig. S5 Supplementary material, http://www.biogeosciences-discuss.net/6/7673/2009/bgd-6-7673-2009-supplement.pdf). In these samples, temporal variation of fluxes of hydrocarbons, alkenones and sterols, mirror the timing of POC fluxes and show no consistent day-night periodicity (Fig. 3). Cholesterol and dehydrocholesterol, markers of zooplankton, and steroid ketones, markers of fecal pellets neither show this diel variability and their flux timing is similar to those of intact phytosterols (Fig. 6). No day-night periodicity is depicted by the present subset of DYNAPROC 2 samples, whilst this periodicity shows on the entire set of samples. Since all biomarkers follow the short-term variability of POC, it is possible that diel variability would have been as significant for biomarkers as it is for POC if the entire dataset (74 samples) had been analyzed for biomarkers.

Two processes can be responsible for the pulses in biomarker flux: changes in the

Full Screen / Esc

magnitude of particle flux (mass flux) and changes in the concentration of biomarkers in the particles. All biomarkers show concurrent variation pattern, and their fluxes are significantly correlated (Table 7). This indicates that a common driver controls biomarker fluxes: the mass flux intensity. Processes controlling aggregation and formation of organic particles have the most driving influence on flux variability. Linear correlations between fluxes of phytoplanktonic biomarkers and those of biomarkers of oxidation, of zooplankton and of higher plants explain a lower fraction of the variance (40 to 65%) than correlations between phytobiomarkers only (Table 7). Notwithstanding the general similar pattern of export, these results indicate some divergence in the relative variation of fluxes of higher plants, of zooplanktonic and phytoplankton constituents. Such divergence implies changes theses constituents within particles, ie changes in their concentrations. Concentrations of biomarker are calculated by normalizing their abundances to that of organic carbon (OC). They vary on a smaller relative magnitude than do export fluxes (Figs. S5 and S6, supplementary material, http://www.biogeosciences-discuss.net/6/7673/2009/bgd-6-7673-2009-supplement.pdf). As a consequence, biomarker concentration changes cause smaller variations of biomarker flux than do organic carbon flux. Interestingly, concentrations of biomarkers are less significantly correlated between themselves than do their fluxes. Concentrations of C37 alkenones and dinosterol are not significantly correlated, neither concentrations of C37 alkenones and higher plant alkanols and alkanes, suggesting that their sources have independent timing (Supplementary material, Table S1). In contrasts, concentration of other biomarkers such as brassicasterol are significantly correlated with concentration of compounds of a distinct origin (Higher plants alkanols and alkanes), suggesting that compositional changes coincide with an unknow common driver.

Drifting sediment trap efficiency may be a drawback to flux estimates. The comparison of thorium export fluxes measured by sediment traps to thorium flux estimated from the deficiency between particulate and dissolved thorium indeed showed discrepancy during the present study (Schmidt et al., 2009). However both estimates considered

distinct depths, and organic carbon mineralization between 60 and 200 m depth may in part explain this discrepancy (Schmidt et al., 2009). The relative abundance of steroid ketones indicates that the exported particles are rather degraded and mostly composed of fecal matter. The ratio of phaeopigments to chlorophyll also supports this view (Marty et al., 2009), together with the concurrent variability of biomarker fluxes and phaeopigment fluxes (Fig. S4 Supplementary material). The high frequency pulses in flux of biomarkers may be triggered by changes in grazing activity. Zooplankton was dominated by copepods during DYNAPROC 2 and their abundance show important short-term variability (Mousseau et al., 2009). Biomass integrated from the surface to 200 m show maximal values at night between the 25 and the 29 September, when maxima in biomarker fluxes also occurred. Relatively high biomass is also observed on the 21 September and the 5 October when biomarker export describes moderate peaks (Mousseau et al., 2009; Fig. 5). Despite these correspondences, the relationship between export fluxes and zooplankton biomass is not always straightforward, for instance very high biomass on the night of the 11 and 13 October contrasts with low export between the 12 and 14 October. The complexity of the coupling between primary production and export also shows when comparing integrated primary production and export fluxes (Fig. 5). Whilst primary production shows little variation between the 17 September and the 5 October, biomarker fluxes remain low during several successive days and describe jagged pulses of high export during others (Fig. 5). After the October wind events and the mixing of the upper water column of (10 October onwards), the production decrease is echoed by minima in the export of biomarkers. Biomarker concentrations normalized to organic carbon points to slight changes in the particle characteristics, in relation to those exported when the water column was still stratified (Fig. S6 Supplementary material, http://www.biogeosciences-discuss.net/6/7673/2009/bgd-6-7673-2009-supplement.pdf). The higher abundance of oxidation indicators (steroid ketones) and of zooplanktonic indicator (cholesterol) and in hydrocarbons, less labile than other lipids, likely reflect a more degraded state of the exported material.

Exported fluxes of biomarkers and the coupling between primary production and ex-port fluxes show considerable variability on short time scale with no obvious relation-ship to wind events. However, the fingerprint of higher plants becomes higher during the first intrusion of coastal waters (Fig. 2) showing these waters and/or the rain sup-ply additional higher plant organic particles, entrained into the rain of sinking particles. Enhanced export of higher plant *n*-alkanes is not triggered by the second intrusion of coastal water, weaker in intensity.

5   Conclusions

The suite of identified biomarkers fingerprints mostly phytoplanktonic and zooplank-tonic remains in the exported material, whilst the higher plant molecular signature is tenuous. The abundance of steroid ketones, oxidation products of sterols is coherent with an important fraction of fecal pellets in the exported material, in good agreement with information brought by pigments and lipid classes on the same samples (Marty et al., 2009).

Lipid biomarker composition points to the dominance of haptophytes over dinoflagel-lates in the exported material, and to a minor contribution of diatoms and eustigmato-phytes. This composition reflects the composition of the phytoplankton in the water col-umn (Marty et al., 2008; Lasternas et al., 2008). Improving our knowledge on sterols of pelagophytes and prochlorophytes, two dominant groups during the late summer situation, would elucidate the contribution of these algae to the remarkable abundance of C29 sterols. Such information will be fundamental to future paleooceanographic studies addressing the Mediterranean sea and other oligotrophic environments.

High frequency sampling of biomarkers exported at 200 m shows a variation range of the same magnitude as seasonal variation. Synchronous timing in fluxes of biomarkers associated with different sources of organic matter strongly suggests that the short term temporal variability depends primarily on physical constrains exerted by particle dynamics, and to lower extend, by particle composition.

Short scale temporal variation of sinking fluxes

L. Méjanelle and J. Dachs

Full Screen / Esc

Printer-friendly Version

Interactive Discussion

CNRS **INSU**
Institut national des **sciences** de **l'Univers**

References

Andersen, V., Goutx, M., Prieur, L., and Dolan, J. R.: Short-scale temporal variability of physical, biological and biogeochemical processes in the NW Mediterranean Sea: an introduction, Biogeosciences, 6, 453–461, 2009,
http://www.biogeosciences.net/6/453/2009/.
Alves, C., Oliveira, T., Pio, C., Silvestre, A. J. D, Fialho, P., Barata, F., and Legrand, M.: Characterisation of carbonaceous aerosols from the Azorean Island of Terceira, Atmos. Environ., 41, 1359–1373, 2007.
Béthoux, J.-P. and Prieur, L.: Hydrologie et circulation en Méditerranée Nord-Occidentale, Pétroles et Techniques, 299, 25–34, 1983.
Bligh, E. G. and Dyer, W. J.: A rapid method of total lipid extraction and purification, Can. J. Biochem. Physiol., 37, 911–917, 1959.
Budge, S. M. and Parrish, C. C.: Lipid biogeochemistry of plankton, settling matter and sediments in Trinity Bay, Newfoundland. II. Fatty Acids, Org. Geochem., 29(5), 1547–1559, 1998.
Burns, K. A., Greenwood, P., Benner, R., Summons, R. S., and Brunskill, G. J.: Vertical fluxes

Short scale temporal variation of sinking fluxes

L. Méjanelle and J. Dachs

|◄ | ►|

◄ | ►

Back | Close

Full Screen / Esc

Printer-friendly Version

Interactive Discussion

of hydrocarbons on the Northwest Shelf of Australia as estimated by a sediment trap study, Org. Geochem., 32, 1241–1255, 2001.

Burns, K. A., Greenwood, P., Benner, R., Brinkman, D., Brunskill, G. J., Codi, S., and Zagorskis, I.: Organic biomarkers for tracing carbon cycling in the Gulf of Papua (Papua New Guinea), Cont. Shelf. Res., 24, 2373–2394, 2003.

Christodoulou, S., Marty, J.-C., Miquel, J.-C., Volkman, J. K., and Rontani, J.-F.: Use of lipids and their deradation products as biomarkers for carbon cycling in the northwestern Maditerranean Sea, Mar. Chem., 113, 25–45, 2009.

Clark, R. C. and Blumer, M.: Distribution of *n*-parafins in marine organisms and sediments, Linol. Oceanogr., 12, 79–87, 1967.

Conte, M. H., Volkman, J. K., and Eglinton, G.: Lipid biomarkers of the Haptophyta, in: The Haptophyte Algae, edited by: Green, J. C. and Leadbeater, B. S. C., Systematics Association Special volume, 51, 351–377, 2004.

Conte, M. H., Eglinton, G., and Madureira, L. A. S.: Long-chain alkenones and alkyl alkenoates as paleotemperature indicators: their production, flux and early sedimentary diagenesis in the Eastern North Atlantic. Org. Geochem., 19, 287–298, 1992.

Cripps, G. C.: Hydrocarbons in the seawater and pelagic organisms of the Soutehrn Ocean, Polar Biol., 10, 393–402, 1990.

Dachs, J., Bayona, J. M., Fowler, S. W., Miquel, J.-C., and Albaigés, J.: Evidence for cyanobacterial inputs and heterotrophic alteration of lipids in sinking particles in the Alboran Sea (SW Mediterranean), Mar. Chem., 60, 189–201, 1998.

Davis, J. B.: Paraffinic hydrocarbons in the sulfate-reducing bacterium *Desulfovibrio desulfuricans*, Chem. Geol., 3, 155–160, 1968.

Dunstan, G. A., Brown, M. R., and Volkman, J. K.: Cryptophyceae and rhodophyceae; chemotaxonomy, phylogeny, and application, Phytochem., 66, 2557–2570, 2005.

Eglinton, G. and Hamilton, R. J.: Leaf epicutilar waxes, Science, 156, 1322–1335, 1967.

Gelin, F., Volkman, J. K., de Leeuw, J. W., and Sinninghe Damsté, J. S.: Midchain hydroxy long-chain fatty acids in microalgae from the genus *Nannochloropsis*, Phytochem., 45, 641–646, 1997.

Goad, L. J. and Whithers, N.: Identification of 27-nor-(24R)-24-methylcholesta-5,22-dien-3β-ol and brassicasterol as the major sterols of the marine dinoflagellate *Gymnodinium simplex*, Lipids, 17, 853–858, 1982.

Goutx, M., Momzikoff, A., Striby, L., Andersen, V., Marty, J.-C., and Vescovali, I.: High-

Short scale temporal variation of sinking fluxes

L. Méjanelle and J. Dachs

Title Page

Abstract | Introduction

Conclusions | References

Tables | Figures

◄ | ►►

◄ | ►

Back | Close

Full Screen / Esc

Printer-friendly Version

Interactive Discussion

frequency fluxes of labile compounds in the central Ligurian Sea, northwestern Mediterranean, Deep-Sea Res. I, 47, 533–556, 2000.

Grimalt, J. O. and Albaigés, J.: Sources and occurrence of C12 –C22 n-alkane distributions with even carbon number preference in sedimentary environments, Geochim. Cosmochim. Acta, 51, 1379–1384, 1987.

Grimalt, J. O., Simoneit, B. R. T., Gómez-Belichón, J. I., Fisher, K., and Dymond, J.: Ascending and descending fluxes of lipid compounds in North atlantic and North Pacific abyssal waters, Nature, 345, 147–150, 1990.

Grimalt, J. O., Calvo, E., and Pelejero, C.: Sea surface paleotemperature errors in UK$'_{37}$ estimation due to alkenone measurements near the limit of detection, Paleoceanography, 16, 226–232, 2001.

Guieu, C., Bozec, Y., Blain, S., Ridame, C., Sarthou, G., and Leblond, N.: Impact of high Saharan dust inputs on dissolved iron concentrations in the Mediterranean Sea, Geophys. Res. Lett., 29(19), 1911, doi:10.1029/2001GL014454, 2002.

Han, J. and Clavin, M.: Hydrocarbon distribution of algae and bacteria, and microbiological activity in sediments, Proc. Natl. Acad. Sci. USA, 64, 436–443, 1969.

Harvey, H. R., Eglinton, G., O'Hara, S. C., and Corner, E. D. S.: Biotransformation and assimilation of dietary lipids by $Calanus$ feeding on a dinoflagellate, Geochim. Cosmochim. Acta, 51, 3031–3040, 1987.

Hinrichs, K.-U., Summons, R. E., Orphan, V., Sylva, S. P., and Hayes, J. M.: Molecular and isotopic analysis of anaerobic methane-oxidizing communities in marine sediments, Org. Geochem., 31, 1685–1701, 2000.

Jetter, R. and Riederer, M.: Long-chain alkanediols, ketoaldehydes, ketoalcohols and ketoalkyl esters in the cuticular waxes of $Osmunda regalis$ fronds, Phytochem., 52, 907–915, 1999.

Kawamura, K., Ishimura, Y., and Yamazaki, K.: Four years' observations of terrestrial lipid class compounds in marine aerosols from the western North Pacific, Global Biogeochem. Cycles, 17(1), 3-1–3-19, doi:10.1029/2001GB001810, 2003.

Körtzinger, A., Schulz-Bull, D. E., Petrick, G., and Duinker, J. C.: Evidence for dissolution of fatty acids in sediment traps: Impact on flux estimates, J. Geophys. Res., 99(C2), 3407–3415, 1994.

Lasternas, S., Tunin-Ley, A., Ibañez, F., Andersen, V., Pizay, M.-D., and Lemée, R.: Dynamics of microphytoplankton abundance and diversity in NW Mediterranean Sea during late summer condition (DYNAPROC 2 cruise; September–October 2004), Biogeosciences Discuss., 5,

Short scale temporal variation of sinking fluxes

L. Méjanelle and J. Dachs

Title Page

Abstract | Introduction

Conclusions | References

Tables | Figures

⏮ | ⏭

◀ | ▶

Back | Close

Full Screen / Esc

Printer-friendly Version

Interactive Discussion

5163–5202, 2008,
http://www.biogeosciences-discuss.net/5/5163/2008/.

Mansour, M. P., Volkman, J. K., and Blackburn, S. I.: The effect of growth phase on the lipid class, fatty acid and sterol composition in the marine dinoflagellate *Gymnodinium* sp. in batch culture, Phytochem., 63, 145–153, 2003.

Marty, J.-C., Nicolas, E., Miquel, J.-C., and Fowler, S. W.: Particulate fluxes of organic compounds and their relationship to zooplankton fecal pellets in the northwestern Mediterranean Sea, Mar. Chem., 46, 387–405, 1994.

Marty, J. C., Garcia, N., and Raimbault, P.: Phytoplankton dynamics and primary production under late summer conditions in the NW Mediterranean Sea, Deep Sea Res. I, 55, 1131–1149, 2008.

Marty, J. C., Goutx, M., Guigue, C., Leblond, N., and Raimbault, P.: Short-term changes in particulate fluxes measured by drifting sediment traps during end summer oligotrophic regime in the NW Mediterranean Sea, Biogeosciences Discuss., 6, 575–606, 2009,
http://www.biogeosciences-discuss.net/6/575/2009/.

Méjanelle, L., Sanchez-Gargallo, A., Bentaleb, I., and Grimalt, J. O.: Long chain *n*-alkyl diols, hydroxy ketones and sterols in a marine eustigmatophyte, *Nannochloropsis gaditana*, and in *Brachionus plicatilis* feeding on the algae, Org. Geochem. 34, 527–538, 2003.

Matsueda, H. and Handa, N.: Vertical flux of hydrocarbons as measured in sediment traps in the eastern north Pacific Ocean, Mar. Chem., 20, 179–195, 1986.

Migon, C., Sandroni, V., and Béthoux, J.-P.: Atmospheric input of anthropogenic phosphorus to the northwest Mediterranean during the oligotrophic season, Marine Environ. Res., 52(5), 413–426, 2001.

Mousseau, L., Lefevre, D., Narcy, F., Nival, P., and Andersen, V.: A one-month study of the zooplankton community at a fixed station in the Ligurian Sea: the potential impact of the species composition on the mineralization of organic matter, Biogeosciences Discuss., 6, 995–1019, 2009,
http://www.biogeosciences-discuss.net/6/995/2009/.

Nichols, P. D., Volkman, J. K., Hallegraeff, G. M., and Blackburn, S. I.: Sterols and fatty acids of the red tide flagellates *Heterosigma akashiwo* and *Chattonella antiqua* (Raphidophycea), Phytochem., 26, 2537–2541, 1987.

O'Neill, L. P., Benitez-Nelson, C. R., Styles, R. M., Tappa, E., and Thunell, R. C.: Diagenetic effects on particulate phosphorus samples collected using formalin-poisoned sediments traps,

Short scale temporal variation of sinking fluxes

L. Méjanelle and J. Dachs

Limnol. Oceanogr. Methods, 3, 308–317, 2005.

Parrish, C. C., Eadies, B. J., Gardner, W. S., and Cavaletto, J. F.: Lipid class and alkane distribution in settling particles of the upper Laurentian Great Lakes, Org. Geochem., 18, 33–40, 1992.

5 Piretti, M. V., Pagliuca, G., Boni, L., Pistocchi, R., Diamante, M., and Gazotti, T.: Investigation of 4-methyl sterols from cultured algal strains, J. Phycol., 33, 61–67, 1997.

Prahl, F. G., Muehlhausen, L. A., and Zahnle, D. I.: Further evaluation of long-chain alkenones as indicators of paleoceanographic conditions, Geochim. Cosmochim. Acta, 52, 2303–2310, 1988.

10 Prahl, F. G., Dymond, J., and Sparrow, M. A.: Annual biomarker record for export production in the central Arabian Sea, Deep-Sea Res. II, 47, 1581–1604, 2000.

Raybaud, V., Nival, P., Mousseau, L., Gubanova, A., Altukhov, D., Khvorov, S., Ibañez, F., and Andersen, V.: Short term changes in zooplankton community during the summer-autumn transition in the open NW Mediterranean Sea: species composition, abundance and diver-

15 sity, Biogeosciences, 5, 1765–1782, 2008, http://www.biogeosciences.net/5/1765/2008/.

Rosell-Melé, A., Comes, P., Müller, P. J., and Ziveri, P.: Alkenone fluxes and anomalous UK$'_{37}$ values during 1989–1990 in the Northest Atlantic (48° N 21° W), Mar. Chem., 71, 251–264, 2000.

20 Sicre, M.-A., Ternois, Y., Miquel, J.-C., and Marty, J.-C.: Alkenones in the Northwestern Mediterranean Sea: interannual variability and vertical transfer, Geophys. Res. Lett., 26(12), 1735–1738, 1999.

Sikes, E. L., O'Leary, T., Nodder, S. D., and Volkman J. K.: Alkenone temperature records and biomarker flux at the subtropical front of the chatham rise, SW Pacific Ocean, Deep-Sea

25 Res., 52, 721–748, 2005.

Sinninghe Damsté, J. S., Kuypers, M., Schouten, S., Schulte, S., and Rullkötter, J.: The lyco-pane/C31 n-alkane ratio as a proxy to assess palaeoxicity during sediment deposition, Earth Planet. Sci. Lett., 209, 215–226, 1993.

Steward, G., Cochran, J. K., Miquel, J. C., Masqué, P., Szlosek, J., Rodriguez y Baena, A. M.,

30 Fowler, S. W., Gasser, B., and Hirschberg, D. J.: Comparing POC export from ^{234}Th/^{238}U and ^{210}Po/^{210}Pb disequilibria with estimates from sediment traps in the northwest Mediterranean, Deep-Sea Res. I, 54, 1549–1570, 2007.

Summons, R. E., Bradley, A. S., Jahnke, L. L., and Waldbauer, J. R.: Steroids, triterpenoids

Short scale temporal variation of sinking fluxes

L. Méjanelle and J. Dachs

Title Page

Abstract	Introduction
Conclusions	References
Tables	Figures

|◀ | ▶|

◀ | ▶

Back | Close

Full Screen / Esc

Printer-friendly Version

Interactive Discussion

and molecular oxygen, Phil. Trans. R. Soc. B, 361, 951–968, doi:10.1098/rstb.2006.1837, 2006.

Ternois, Y., Sicre, M.-A., Boireau, A., Mart, J.-C., and Miquel, J.-C.: Production pattern of alkenones in the Mediterranean Sea, Geophys. Res. Lett., 23(22), 3171–3174, 1996.

5 Ternois, Y., Sicre, M.-A., Boireau, A., Conte, M. H., and Eglinton, G.: Evaluation of long-chain alkenones as paleo-temperature indicators in the Mediterranean Sea, Deep-Sea Res., 44, 271–286, 1997.

Ternois, Y., Sicre, M.-A., Boireau, A., Beaufort, L., Miquel, J.-C., and Jeandel, C.: Hydrocarbons, sterols and alkenones in sinking particles in the Indian Ocean sector of the Southern

10 Ocean, Org. Geochem., 28, 489–501, 1998.

Tolosa, I., Leblond, N., Copin-Montaigut, C., Marty, J.-C., de Mora, S., and Prieur, L.: Distribution of sterol and fatty alcohol biomarkers in particulate matter from the frontal structure of the Alboran Sea (S.W. Mediterranean Sea), Mar. Chem., 82, 161–183, 2003.

Tolosa, I., Leblond, N., Marty, J.-C., de Mora, S., and Prieur, L.: Export fluxes of organic carbon

15 and lipid biomarkers from the frontal structure of the Alboran Sea (SW Mediterranean Sea) in winter, J. Sea Res., 54, 125–142, 2005.

Versteegh, G. J. M., Jansen, J. H. F., de Leeuw, J. W., and Schneider, R. R.: Mid-chain diols and keto-ols in SE Atlantic sediments: A new tool for tracing past sea surface water masses?, Geochim. Cosmochim. Acta, 11, 1879–1892, 2000.

20 Villanueva, J. and Grimalt, J. O.: Pitfalls in the chromatographic determination of the alkenone UK'_{37} index for paleotemperature estimation, J. Chromatogr. A, 723, 285–291, 1996.

Volkman, J. K.: A review of sterol markers for marine and terrigeneous matter, Org. Geochem., 9, 83–99, 1986.

Volkman, J. K., Johns, R. B., Gillian, F. T., and Perry, G. J.: Microbial lipids of an intertidal

25 sediment. Geochim. Cosmochim. Acta, 44, 1133–1143, 1980.

Volkman, J. K., Barrett, S. M., Dunstan, G. A., and Jeffrey, S. W.: C30-C32 alkyl diols and unsaturated alcohols in microalgae of the class Eustigmatophyceae, Org. Geochem., 18(1), 131–138, 1992.

Volkman, J. K., Barrett, S. M., Dunstan, G. A., and Jeffrey, S. W.: Geochemical significance of

30 the occurrence of dinosterol and other 4-methyl sterols in a marine diatom, Org. Geochem., 20(1), 7–15, 1993.

Volkman, J. K., Barrett, S., and Blackburn, S.: Eustigmatophyte microalgae are potential sources of C29 n-alcohols and C28-C32 n-alkyl diols in freshwater environments, Org.

Short scale temporal variation of sinking fluxes

L. Méjanelle and J. Dachs

Title Page

Abstract | Introduction

Conclusions | References

Tables | Figures

⏮ | ⏭

◀ | ▶

Back | Close

Full Screen / Esc

Printer-friendly Version

Interactive Discussion

Geochem., 30, 307–318, 1999.

Volkman, J. K., Barrett, S., Blackburn, S., Mansour, M., Sikes, E., and Gelin, F.: Microalgal biomarkers: A review of recent research developments, Org. Geochem., 29, 1163–1179, 1998.

5 Wang, G., Kawamura, K., and Lee, M.: Comparison of organic compositions in dust storm and normal aerosol samples collected at Gosan, Jeju Island, during spring 2005, Atmos. Environ., 43, 219–227, 2009.

Wakeham, S. G. and Canuel, E. A.: Lipid composition of the pelagic crab *Pleuroncodes planipedes*, its feces and sinking particulate organic matter in the equatorial North Pacific Ocean,
10 Organic Geochemistry, 9, 331–343, 1986.

Wakeham, S. G. and Canuel, E. A.: Organic geochemistry of particulate matter in the eastern tropical North Pacific Ocean: Implications for particle dynamics, J. Mar. Res., 46, 183–213, 1988.

Wakeham, S. G. and Lee, C.: Organic geochemistry of particulate matter in the ocean: The
15 role of particles in oceanic sedimentary cycles, Org. Geochem., 14, 83–96, 1989.

Wakeham, S. G. and Beier, J. A.: Fatty acids and sterol biomarkers as indicators of particulate matter source and alteration processes in the Black Sea, Deep-Sea Res., 38, S943–S968, 1991.

Wakeham, S. G., Peterson, M. L., Hedges, J. I., and Lee, C.: Lipid biomarker fluxes in the
20 Arabian Sea, with a comparison to the equatorial Pacific Ocean, Deep-Sea Res. II, 49, 2265–2301, 2002.

Wakeham, S. G., Lee, C., Peterson, M. L., Liu, Z., Szlosek, J., Putman, I. F., and Xue, J.: Organic biomarkers in the twilight zone – series and settling velocity sediment traps during MedFlux, Deep-Sea Res. II, 56(18), 1437–1453, doi:10.1016/j.dsr2.2008.11.030, 2009.

Short scale temporal variation of sinking fluxes

L. Méjanelle and J. Dachs

Title Page

Abstract	Introduction
Conclusions	References
Tables	Figures

|◄ | ►|

◄ | ►

Back | Close

Full Screen / Esc

Printer-friendly Version

Interactive Discussion

Table 1. Positions and dates of mooring and recovering of drifting sediment traps.

Series of samples	A	B	C	D
Mooring location	43°24.80 N 8°00.61 E	43°23.06 N 8°01.52 E	43°23.59 N 8°02.78 E	43°23.79 N 8°00.36 E
Recovering location	43°22.72 N 7°51.75 E	43°18.68 N 8°04.93 E	43°19.31 N 7°46.09 E	43°25.36 N 8°00.18 E
Date	17–22 September 2004	24–29 September 2004	3–8 October 2004	10–15 October 2004
Mass Flux in $mg\,m^{-2}\,d^{-1}$	3.17±0.01	1.73±0.01	2.41±0.01	0.95±0.01

Title Page

Abstract | Introduction

Conclusions | References

Tables | Figures

◄◄ | ►►

◄ | ►

Back | Close

Full Screen / Esc

Printer-friendly Version

Interactive Discussion

Table 2. Hydrocarbon composition of sinking particles collected by drifting sediment traps, in percent of identified hydrocarbons, and total hydrocarbon flux. n.d.: non detected. [a] Hydrocarbon fractions of three samples were lost.

Date	17 Sep			18 Sep		21 Sep					28 Sep				29 Sep		3 Oct		4 Oct				5 Oct			12 Oct	13 Oct				14 Oct
Starting time (hours)	8	14	20	2	8	2[a]	8	14	20	2[a]	2	8	14	20	2	8	14	20	2	8	14	20	2	8	14[a]	20	2	8	14	20	2
Compounds:																															
C_{12}	n.d.	n.d.	n.d.	6.7	15.3		n.d.	n.d.	9.8		n.d.	3.0	1.4	1.0	3.5	n.d.	n.d.	n.d.	n.d.	n.d.	n.d.	n.d.	n.d.	n.d.		n.d.	n.d.	n.d.	n.d.	n.d.	n.d.
C_{13}	n.d.	n.d.	n.d.	n.d.	0.2		n.d.	10.5	0.2		n.d.	n.d.	n.d.	0.4	n.d.	n.d.	n.d.	n.d.	n.d.	n.d.	n.d.	n.d.	n.d.	n.d.		n.d.	n.d.	n.d.	n.d.	n.d.	n.d.
C_{14}	n.d.	n.d.	n.d.	n.d.	n.d.		n.d.	n.d.	1.1		n.d.	0.7	n.d.	n.d.	n.d.	n.d.	3.3	1.7	2.4	0.6	1.9	0.7	0.6	0.8		4.9	4.3	1.7	1.1	1.3	1.8
C_{15}	0.8	0.7	1.9	2.9	1.2		1.9	1.3	0.4		n.d.	3.4	0.9	0.9	n.d.	2.7	3.3	1.7	4.3	1.2	2.3	1.9	2.3	0.8		7.5	29.0	4.0	4.2	2.5	2.5
C_{16}	2.2	1.6	3.5	4.0	1.3		1.9	2.0	0.8		2.9	2.9	1.6	0.8	1.9	3.2	6.8	3.4	4.3	1.2	2.3	1.9	2.9	1.5		5.2	4.5	2.3	1.8	1.3	1.7
C_{17}	0.8	0.8	3.2	4.0	1.5		3.0	2.8	2.1		1.6	3.0	2.1	1.1	2.0	2.9	1.5	3.0	3.1	1.8	2.1	2.0	2.9	1.5		5.2	4.5	2.3	1.8	1.3	1.7
pristane	n.d.	1.0	2.7	n.d.	1.2		2.2	3.4	1.3		2.5	2.6	2.1	2.0	1.7	1.3	n.d.	1.6	1.8	n.d.	1.3	1.0	2.2	1.0		2.1	1.4	3.5	3.3	0.7	n.d.
C_{18}	2.5	2.9	5.4	4.7	1.9		5.4	5.3	7.0		4.6	4.3	2.6	2.0	2.3	3.4	6.0	5.2	5.5	3.3	4.8	3.0	3.6	2.3		6.3	4.3	6.2	7.1	2.8	3.8
Phytane	1.0	0.4	1.0	n.d.	0.9		1.4	1.5	1.2		2.2	n.d.	1.2	1.2	1.6	1.1	n.d.	0.8	0.9	0.7	n.d.	0.6	1.6	0.4		1.0	n.d.	0.4	1.4	0.3	1.5
C_{20}	9.1	7.9	7.6	11.4	7.8		16.8	11.1	15.0		12.6	8.7	3.4	4.0	4.8	5.3	4.6	8.5	10.0	9.3	11.4	7.8	6.2	6.5		9.6	6.2	7.0	9.4	13.6	15.3
C_{21}	5.1	3.5	6.2	8.5	3.9		10.6	8.4	9.2		5.9	6.8	2.9	3.5	6.8	4.0	8.5	5.4	6.7	7.4	7.8	6.3	5.3	6.2		6.9	4.6	2.9	3.8	12.3	14.2
C_{22}	7.0	5.9	6.1	5.2	3.0		5.0	6.5	4.3		5.3	5.0	2.9	2.9	5.9	3.3	2.7	7.0	9.0	6.3	8.2	7.1	7.0	6.9		5.5	4.6	6.0	8.7	8.1	9.7
C_{24}	4.9	5.2	3.3	5.2	15.7		1.8	3.0	1.1		6.4	4.8	2.1	2.6	3.3	1.5	33.6	5.6	6.6	3.0	5.0	5.3	5.2	5.0		5.0	4.4	5.0	7.5	3.1	3.1
C_{25}	4.0	2.3	2.7	4.5	12.8		5.5	2.7	1.5		3.8	2.3	4.0	3.0	2.8	3.4	9.2	2.5	2.8	2.9	2.9	2.9	1.8	4.1		3.4	3.8	1.8	2.1	1.9	6.8
C_{26}	3.9	4.5	2.5	0.9	0.7		0.9	0.8	0.6		1.9	2.1	1.3	1.1	n.d.	0.8	0.6	2.1	2.5	1.7	2.3	1.9	1.9	1.9		2.1	2.9	3.4	4.3	2.4	1.7
Squalane	14.9	9.8	11.0	2.5	2.4		3.0	3.4	5.1		11.1	11.6	4.4	1.7	4.8	4.0	n.d.	4.3	5.4	10.4	12.0	6.1	3.9	12.4		4.7	0.9	13.4	16.5	7.5	8.5
C_{27}	4.5	6.4	4.5	6.3	2.3		9.2	4.6	4.4		5.4	5.1	8.9	10.2	6.9	9.2	3.2	5.9	4.7	4.8	4.8	6.9	8.9	8.1		3.7	3.9	2.4	3.0	3.7	2.2
C_{28}	3.7	4.8	2.9	1.5	1.1		1.2	0.9	1.1		2.0	2.1	1.7	1.6	1.6	1.3	1.7	1.9	2.0	1.9	1.7	1.9	1.8	1.9		1.4	2.4	6.9	3.9	2.7	1.9
Squalene	13.5	11.7	12.9	7.3	4.5		2.1	2.6	4.1		7.0	7.6	13.5	5.8	16.9	13.4	5.2	22.5	11.8	23.9	6.2	11.3	11.8	9.4		14.7	5.6	17.2	4.0	12.2	14.3
C_{29}	2.8	3.6	5.4	5.3	4.1		8.8	12.2	7.5		6.7	6.9	15.0	18.0	12.3	13.1	1.9	8.1	6.7	7.2	9.3	11.3	12.7	12.2		4.1	5.0	2.4	2.8	6.0	3.3
C_{30}	3.9	4.6	3.0	1.2	0.7		0.9	1.1	1.1		2.0	2.0	1.2	1.4	n.d.	1.1	3.8	1.4	1.9	1.7	2.2	2.9	2.9	0.7		1.3	2.8	2.8	3.5	2.5	2.5
C_{31}	2.8	3.2	3.6	3.4	2.6		4.0	5.2	4.0		3.4	3.4	6.5	8.1	5.0	6.5	0.8	2.8	3.9	3.6	4.9	5.2	4.0	3.1		3.9	4.4	3.0	4.6	4.2	1.6
C_{32}	2.0	2.7	1.7	0.9	1.8		0.4	n.d.	0.8		1.7	n.d.	n.d.	n.d.	n.d.	n.d.	2.7	0.9	1.3	1.2	1.3	1.1	0.8	0.9		0.7	1.5	2.2	n.d.	2.2	0.8
Diploptene	n.d.	n.d.	n.d.	n.d.	1.0		tr	n.d.	0.3		n.d.	n.d.	0.4	0.6	n.d.	n.d.	n.d.	0.3	n.d.	n.d.	n.d.	0.7	n.d.	0.8		n.d.	n.d.	n.d.	2.4	n.d.	n.d.
C_{33}	1.6	1.8	2.1	1.4	1.1		0.8	1.6	1.5		1.4	2.0	2.5	2.6	1.9	2.1	3.8	1.1	1.6	1.7	1.7	3.5	1.5	2.1		1.4	1.7	2.0	1.8	2.7	0.9
C_{34}	1.1	1.4	0.8	n.d.	n.d.		0.4	n.d.	0.4		n.d.	n.d.	n.d.	n.d.	n.d.	n.d.	n.d.	0.6	0.6	0.9	n.d.	0.7	n.d.	n.d.		n.d.	0.5	1.3	1.5	1.4	n.d.
Lycopane	0.8	0.8	0.9	1.1	0.6		2.2	2.2	1.4		n.d.	n.d.	2.3	2.9	1.7	2.1	n.d.	1.1	1.5	1.6	3.4	2.1	0.4	2.6		0.3	n.d.	0.3	0.5	0.7	1.5
C_{35}	0.4	0.8	0.9	n.d.	1.3		0.4	n.d.	0.5		n.d.	n.d.	n.d.	n.d.	n.d.	0.9	n.d.	0.6	0.5	0.5	n.d.	0.6	0.3	0.7		1.6	0.9	0.4	0.8	0.9	0.2
C_{36}	n.d.	n.d.	0.5	n.d.	n.d.		n.d.	n.d.	0.6		n.d.	n.d.	n.d.	n.d.	n.d.	n.d.	n.d.	0.4	n.d.	n.d.	n.d.	1.0	n.d.	n.d.		n.d.	n.d.	n.d.	n.d.	1.4	n.d.
$C_{37:3}$	2.3	4.2	2.6	6.9	5.0		7.4	6.7	8.8		5.9	6.6	9.0	12.1	6.9	9.0	n.d.	1.2	2.4	1.9	2.6	3.2	7.9	5.1		1.5	0.4	n.d.	n.d.	0.8	n.d.
C_{37}	n.d.	n.d.	n.d.	n.d.	n.d.		n.d.	n.d.	0.3		n.d.	n.d.	n.d.	n.d.	n.d.	n.d.	n.d.	n.d.	n.d.	n.d.	n.d.	1.0	n.d.	n.d.		n.d.	n.d.	n.d.	n.d.	0.5	n.d.
$C_{38:3}$	4.6	7.7	1.0	4.4	4.1		2.7	n.d.	3.1		3.5	2.9	6.0	8.6	5.4	3.3	n.d.	0.2	n.d.	0.6	n.d.	1.1	2.6	1.7		1.3	n.d.	1.6	n.d.	n.d.	n.d.
Total hydrocarbon flux ($\mu\mathrm{g\,m^{-2}\,d^{-1}}$)	5.6	4.9	5.5	5.9	15.8		14.9	8.9	29.7		12.4	9.5	16.3	14.0	9.3	14.3	1.4	7.6	6.7	7.0	4.7	8.5	7.8	9.3		10.2	21.1	9.9	7.0	8.4	8.1

Short scale temporal variation of sinking fluxes

L. Méjanelle and J. Dachs

Title Page

Abstract | Introduction

Conclusions | References

Tables | Figures

|◀ | ▶|

◀ | ▶

Back | Close

Full Screen / Esc

Printer-friendly Version

Interactive Discussion

Table 3. Fluxes of long chain alkenones and alkenoates recorded by drifting sediment traps during the DYNAPROC2 cruise, in μg m^{-2} d^{-1} and values of the alkenone unsaturation index, UK$'_{37}$. Methyl alkenones and ethyl alkanones are designated by the the corresponding prefixes. The OMethyl prefix stands for methyl alkanoate. n.d.: non detected. [a] The UK$'_{37}$ values are not calculated because of the too small peak area of C$_{37:3}$.

Date	17 Sep			18 Sep		21 Sep					28 Sep				29 Sep		3 Oct		4 Oct				5 Oct			12 Oct	13 Oct				14 Oct
Starting time (hours)	8	14	20	2	8	2	8	14	20	2	2	8	14	20	2	8	14	20	2	8	14	20	2	8	14	20	2	8	14	20	2
Compounds:																															
Methyl C37:3	0.1	0.1	0.2	0.4	1.1	1.7	2.5	2.3	4.1	1.9	1.0	0.4	3.7	5.9	0.6	0.3	0.3	0.3	0.2	0.4	0.4	1.1	1.2	1.7	2.6	n.d.	n.d.	n.d.	n.d.	0.1	0.1
Methyl C37:2	0.4	0.7	0.5	0.5	1.6	3.1	4.5	3.7	7.4	3.3	1.2	0.6	4.9	7.4	0.6	0.4	0.8	0.7	0.4	0.7	0.8	2.0	1.6	3.5	4.6	n.d.	n.d.	n.d.	n.d.	0.3	0.3
OMethyl C36:2	n.d.	0.0	0.1	0.1	0.2	0.4	0.6	0.3	1.0	0.2	0.1	0.2	0.4	0.8	0.2	n.d.	n.d.	0.2	n.d.	0.04	0.1	0.1	0.1	n.d.	n.d.	n.d.	n.d.	n.d.	n.d.	n.d.	n.d.
Ethyl C38:3	0.05	0.0	0.2	0.3	0.5	0.8	1.1	1.3	2.7	1.2	0.7	0.02	1.8	3.2	0.1	0.1	0.2	0.2	0.2	0.2	0.3	1.6	0.6	2.1	4.4	n.d.	n.d.	n.d.	n.d.	0.5	0.1
Methyl C38:3	0.03	0.1	0.1	0.0	0.1	1.0	1.3	1.2	2.2	1.0	0.6	0.1	2.2	3.5	0.3	0.2	0.1	n.d.	n.d.	0.2	0.2	0.6	0.7	n.d.	1.7	n.d.	n.d.	n.d.	n.d.	n.d.	0.1
Ethyl C38:2	0.3	0.4	0.5	0.2	0.7	2.4	3.3	3.2	6.1	2.7	1.1	0.1	3.9	6.4	0.3	0.1	0.7	0.7	0.5	1.0	1.1	2.7	2.0	4.2	6.1	n.d.	n.d.	n.d.	n.d.	n.d.	0.2
Methyl C38:2	n.d.	n.d.	n.d.	n.d.	n.d.	1.7	2.7	1.7	3.6	1.6	0.6	0.2	3.1	3.8	0.4	0.2	n.d.	n.d.	n.d.	n.d.	n.d.	n.d.	n.d.	n.d.	n.d.	n.d.	n.d.	n.d.	n.d.	n.d.	n.d.
Methyl C39:3	n.d.	0.03	0.03	0.1	0.2	0.2	0.3	0.3	0.6	0.2	0.1	n.d.	0.4	0.9	n.d.	n.d.	0.03	0.05	0.09	0.1	0.1	0.2	0.2	0.3	0.6	n.d.	n.d.	n.d.	n.d.	n.d.	0.0
Methyl C39:2	0.2	0.1	0.3	0.4	0.3	0.7	1.0	0.9	1.7	0.7	0.3	0.3	1.2	1.8	n.d.	n.d.	0.1	0.3	0.1	0.2	0.3	0.6	0.4	0.9	1.0	n.d.	n.d.	n.d.	n.d.	0.3	0.2
UK$'_{37}$ (RU)	a	a	0.68	0.60	0.59	0.64	0.64	0.62	0.64	0.64	0.55	0.61	0.57	0.56	0.50	0.57	0.75	0.70	0.70	0.66	0.66	0.64	0.57	0.67	0.64					a	0.67

Table 4. Fluxes of sterols, n-alkanols, alkane diol and steroidal ketones in sinking particles collected by drifting sediment traps during the DYNAPROC2 cruise, in $\mu g\,m^{-2}\,d^{-1}$. n.d.: non detected. Sterols are designed by $x\Delta y, z$, where x indicates substituents and their location on the side chain or on the A ring; x can also indicate the 24-nor or 27-nor configuration. In this nomenclature, y and z indicate double bond locations. $\Delta 0$ is used to design 5α-(H)stanols. [a] coeluting with an isomer of cholestan-3β-one in minor amounts. [b] Coeluting with minor amounts of a cholesta-4,22E-dien-3β-one isomer in some samples. [c] coeluting with 24-methylcolesta-5,24(28)-dien-3β-ol. [d] coeluting with 4αt24dimethyl Δ22 in minor amounts. [e] Coeluting with 4α,4β,24-trimethyl Δ0.

Date	17 Sep			18 Sep		21 Sep					28 Sep				29 Sep		3 Oct		4 Oct				5 Oct				12 Oct		13 Oct					14 Oct
Starting time (hours)	8	14	20	2	8	2	8	14	20	2	2	8	14	20	2	8	14	20	2	8	14	20	2	8	14	20	2	14	2	8	14	20	2	2
C22-OH	0.7	0.3	0.1	0.4	0.4	0.4	0.6	0.4	0.9	0.5	0.6	0.5	1.0	1.1	0.4	0.6	n.d.	0.1	0.5	0.4	0.5	0.8	n.d.	0.7	0.6		0.2		0.7	0.3	0.2	0.6		0.4
C24-OH	n.d.	n.d.	0.1	0.6	0.3	0.3	0.5	0.3	0.7	0.3	0.3	0.2	0.6	0.5	0.2	0.4	0.1	0.1	0.1	n.d.	n.d.	n.d.	n.d.	n.d.	0.1		n.d.		0.1	0.1	n.d.	0.0		0.1
C26-OH	0.4	0.1	0.2	0.9	1.5	0.6	0.9	0.5	0.6	0.5	0.3	0.3	1.0	1.3	0.3	0.7	0.1	0.2	0.2	0.1	n.d.	0.5	n.d.	0.4	0.5		0.1		0.3	0.1	0.1	0.3		0.2
24-nor Δ5,22E	0.7	0.8	0.6	1.0	2.1	2.9	4.5	2.8	5.0	2.6	2.4	1.9	4.8	6.4	2.1	3.6	0.9	0.9	1.4	1.4	1.5	2.7	1.8	2.4	3.3		0.7		0.8	0.7	0.3	0.8		0.5
24-nor Δ5	0.2	0.3	0.3	0.4	1.0	0.8	1.5	0.8	1.5	0.6	0.3	0.3	0.8	1.0	0.3	0.7	0.1	0.2	0.2	0.2	0.3	0.3	0.4	0.4	0.6		0.1		0.2	0.2	0.1	0.2		0.1
24-nor-cholesta-4,22E-dienone	0.3	0.1	0.2	0.3	0.7	0.6	1.5	1.2	1.6	1.1	0.7	0.8	2.1	2.4	0.6	1.7	0.2	0.3	0.3	0.6	0.3	1.0	0.2	0.5	0.5		n.d.		0.2	n.d.	n.d.	0.3		0.1
Cholestan-3-one	0.4	0.3	0.3	0.1	0.3	0.3	0.8	0.6	0.8	0.5	n.d.	1.3	0.3	0.3	1.3	0.1	0.5	0.4	1.2	1.1	0.4	n.d.	0.1	0.1	n.d.		0.1		0.1	0.1	n.d.	0.1		0.1
27-nor Δ5,22E	3.6	3.7	3.8	5.5	13.2	16.9	25.8	16.0	29.4	17.1	14.3	11.8	27.6	35.2	11.8	20.3	5.3	4.7	8.5	7.7	8.3	14.5	10.5	13.7	18.2		4.3		6.5	4.0	2.5	4.3		3.5
27-nor Δ5	0.6	1.0	0.9	1.7	4.2	3.6	5.5	3.5	5.8	2.5	1.6	1.5	3.7	5.7	1.6	3.1	0.4	0.4	0.6	0.6	0.7	1.5	1.5	2.9	2.0		0.7		0.8	0.7	0.3	0.6		0.3
Δ5,22E	3.3	3.3	5.2	3.6	9.0	12.0	16.8	10.5	18.1	23.5	11.4	7.6	18.4	21.2	8.4	12.6	6.6	5.3	11.1	8.0	8.6	13.2	7.9	11.7	13.1		3.3		5.8	2.6	1.5	3.6		3.7
Δ22E	0.8	1.7	1.5	1.7	3.5	3.6	5.2	2.9	5.7	2.4	1.9	1.7	4.4	5.6	1.8	3.3	1.4	1.4	1.5	1.5	1.3	3.1	3.2	5.0	3.5		1.3		1.3	0.9	0.5	1.3		0.6
C28-OH	0.1	0.1	0.1	2.9	2.1	1.5	2.5	1.8	0.7	1.0	n.d.	0.4	2.5	7.7	16.7	2.1	n.d.	n.d.	0.6	0.6	n.d.	0.4	n.d.	n.d.	n.d.		0.2		0.7	0.1	0.1	n.d.		n.d.
Δ5	11.5	11.1	9.9	7.2	17.9	18.9	23.7	18.3	47.6	16.5	22.0	13.0	34.6	25.0	3.0	20.3	13.8	12.8	23.3	20.2	21.1	36.6	12.9	22.1	44.4		6.0		10.1	16.4	6.9	21.9		9.6
Δ0[a]	1.3	1.3	2.2	2.1	3.8	4.9	7.0	4.2	8.6	3.8	3.2	2.7	8.4	8.7	0.6	5.2	1.6	1.6	2.2	2.3	2.5	3.6	2.7	4.2	4.2		1.4		1.6	1.3	1.0	1.7		1.1
Δ5,24	0.3	0.2	0.3	1.2	1.4	1.3	1.9	1.2	1.9	0.9	0.8	0.9	1.2	1.8	1.9	1.1	1.6	1.3	1.4	1.7	1.2	1.3	3.2	1.1	3.8		0.3		0.2	0.6	0.3	0.9		n.d.
4αMeΔ24(25)[b]	n.d.	n.d.	n.d.	1.1	1.4	0.9	1.8	2.9	3.5	2.9	1.8	2.5	4.0	5.4	0.7	4.5	0.3	0.3	0.5	0.5	0.4	0.6	0.5	0.9	0.8		0.3		0.9	0.8	0.3	0.5		0.4
Cholesta-4,22E-dien-3-one	0.3	n.d.	0.3	n.d.	n.d.	n.d.	n.d.	n.d.	n.d.	n.d.	n.d.	0.6	n.d.	n.d.	0.2	0.2	0.3	0.3	1.5	n.d.	2.5	2.5	4.2	2.2	0.8		0.2		n.d.	n.d.	n.d.	0.7		0.2
24-Methyl Δ5,22E	6.5	7.6	7.8	12.4	29.5	36.1	52.9	35.4	62.2	38.7	34.1	28.1	65.1	83.0	26.6	51.2	9.8	9.0	17.3	14.5	16.1	27.7	22.7	29.7	39.5		10.6		17.7	10.2	5.1	9.4		8.1
24-MethylΔ22E	1.9	2.3	2.4	2.8	6.9	7.2	10.1	5.4	10.5	4.7	3.4	3.1	13.2	9.9	3.0	8.8	2.7	2.4	2.1	4.8	2.6	7.7	11.3	8.3	6.3		2.2		2.8	1.6	0.9	3.2		1.4
Cholestediol	0.1	0.1	0.1	1.4	0.4	0.1	n.d.	0.2	0.2	0.2	0.1	n.d.	0.3	n.d.	0.1	n.d.	0.4	0.4	0.2	0.2	0.2	n.d.	0.8	0.9	1.0		n.d.		0.0	0.1	0.1	0.4		0.1
Cholest-4-en-3-one	3.8[c]	4.2[c]	4.4[c]	3.4	9.3	6.0	12.3	14.5	17.1	12.6	12.6	14.4	33.8	35.2	11.8	28.8	9.1[c]	8.7[c]	5.6[c]	15.0[c]	7.5[c]	24.1[c]	37.0[c]	20.0[c]	15.0[c]		3.6		4.5	2.3	1.2	11.3[c]		4.2[c]
24-Methyl Δ5,24(28)	n.d.	n.d.	n.d.	2.4	6.2	8.8	11.5	6.8	13.1	6.3	5.1	4.4	15.1	14.5	4.3	10.5	n.d.	n.d.	n.d.	n.d.	n.d.	n.d.	n.d.	6.6	n.d.		2.8		3.5	1.5	0.7	n.d.		0.6
24-Methyl Δ5	0.5	0.9	0.9	1.7	4.0	3.5	5.6	3.9	6.3	3.1	2.1	1.9	4.9	5.3	1.0	3.3	0.8	0.5	0.8	0.7	0.7	0.8	2.3	2.7	0.9		1.0		0.4	0.4	0.2	0.4		0.4
24-MethylΔ5,7,22E	n.d.	n.d.	0.3	0.6	0.6	0.8	0.4	0.9	0.4	0.5	0.4	0.8	0.3	0.4	0.6	n.d.	0.6	0.6	1.6	n.d.	1.3	2.2	0.4	0.3	0.2		0.1		0.3	0.2	0.1	0.6		0.3
23,24-Dimethyl Δ5,22E	0.6	0.7	0.7	1.3	3.3	2.2	4.3	3.5	6.1	2.5	3.0	3.1	5.8	7.9	2.3	3.9	0.9	0.9	1.5	1.8	1.5	3.1	3.0	3.6	4.9		1.4		1.6	1.4	1.2	1.2		0.7
23,24-Dimethyl Δ22E	0.3	0.2	0.2	0.3	1.1	0.8	1.7	2.4	1.3	2.5	1.5	2.1	2.7	2.4	1.3	2.7	0.3	0.3	0.5	0.6	0.7	0.6	0.6	0.3	0.2		0.3		0.2	0.2	0.1	0.3		0.2
24-Ethyl Δ5,22E	1.7	2.1	2.5	3.5	8.6	10.1	15.7	9.3	17.7	11.6	7.9	7.5	20.3	24.7	7.7	5.1	2.5	2.5	5.5	4.6	5.0	11.3	8.8	12.8	15.9		3.8		5.4	4.1	1.9	3.3		2.5
24-Ethyl Δ22E[d]	0.8	1.0	1.0	1.5	3.8	4.1	5.5	3.5	5.5	3.4	2.7	2.8	6.8	8.6	2.3	1.0	2.9	2.7	1.0	3.3	2.9	4.1	8.3	3.1	2.8		1.1		1.1	0.9	0.5	4.5		0.8
24-Methyl Δ7,24(28)	0.1	0.3	0.3	1.2	0.6	0.6	1.2	0.8	2.6	0.9	0.3	0.8	1.3	9.8	1.4	0.6	0.2	0.1	0.2	0.2	0.2	0.4	0.9	1.1	0.7		0.9		0.9	0.1	0.2	0.2		0.1
23,24-dimethyl Δ5	n.d.	n.d.	n.d.	2.4	3.6	2.8	4.1	2.8	3.2	2.5	1.1	1.5	3.9	9.4	1.8	3.5	1.3	1.4	1.5	1.8	1.0	3.0	1.8	3.6	5.2		0.4		0.9	0.6	0.2	1.4		0.4
24-Ethyl Δ5	4.5	4.7	5.2	6.8	17.2	17.8	26.4	17.3	31.0	17.6	14.3	13.5	30.2	38.1	12.7	24.1	4.9	4.8	8.5	7.4	7.6	14.4	11.9	17.1	20.5		5.4		7.2	5.3	3.4	6.0		4.3
24-Ethyl Δ0	0.5	0.4	0.3	1.8	5.5	4.3	7.4	4.6	7.6	4.0	3.1	3.0	7.0	9.0	2.4	6.3	0.6	0.5	0.3	1.3	0.1	1.1	2.2	0.8	1.5		1.4		1.3	1.3	0.8	0.9		0.3
24-Ethyl Δ5,24(28)	1.7	1.8	2.1	1.7	2.2	3.2	3.3	2.1	4.3	2.6	2.4	2.6	5.0	6.8	2.3	3.3	1.8	1.9	3.0	2.3	1.9	4.8	5.2	7.0	7.5		1.1		2.0	1.1	0.7	n.d.		n.d.
4α23,24-Trimethyl Δ22,24(28)	n.d.	n.d.	n.d.	1.0	1.6	1.7	2.5	1.9	3.6	1.4	1.2	1.6	1.3	3.1	0.8	1.6	n.d.	0.1	0.7	0.3	0.3	n.d.	n.d.	n.d.	n.d.		n.d.		0.3	0.2	0.0	3.4		1.8
4α23,24-Trimethyl Δ22	1.1	1.8	1.6	2.0	5.3	5.8	8.4	5.6	10.4	5.5	4.0	4.8	9.9	13.4	4.0	8.0	1.5	1.3	2.1	2.1	1.8	4.1	5.2	6.2	7.2		1.3		1.7	1.4	0.7	1.7		0.9
24-Propyl Δ5,24(28) isomer	n.d.	n.d.	n.d.	0.2	0.2	0.2	0.4	n.d.	0.4	0.1	0.1	n.d.	0.3	0.2	0.1	0.2	n.d.	n.d.	n.d.	n.d.	n.d.	n.d.	n.d.	n.d.	n.d.		n.d.		n.d.	0.0	n.d.	n.d.		n.d.
4α23,24-Trimethyl Δ7	0.1	0.2	0.2	n.d.	n.d.	0.2	n.d.	0.1	0.9	n.d.	0.2	0.2	0.5	0.3	n.d.	n.d.	n.d.	n.d.	0.1	0.3	n.d.	n.d.	n.d.	n.d.	n.d.		n.d.		0.2	0.0	0.0	0.5		0.2
24-Propyl Δ5,24(28)	0.4	0.7	0.7	0.7	2.2	1.8	2.8	1.3	2.4	2.3	2.4	2.9	2.5	4.1	1.5	2.8	0.9	1.0	1.7	1.0	1.8	2.1	5.1	3.7	2.9		0.4		1.3	1.0	0.4	1.1		0.4
4α23,24-Trimethyl Δ7	n.d.	0.1	0.1	n.d.	1.2	1.1	0.7	0.4	0.6	0.2	1.2	1.5	1.0	2.7	1.0	2.0	0.2	0.1	0.1	0.3	n.d.	n.d.	n.d.	0.5	0.7		0.1		0.6	0.5	0.3	0.2		0.2
4α23,24-Trimethyl Δ5[e]	0.4	0.4	0.4	0.4	1.2	1.0	1.0	0.7	1.5	0.5	0.8	0.8	1.4	0.5	0.9	0.4	0.3	0.5	0.7	0.9	0.5	1.3	0.5	1.3	1.3		0.3		0.3	0.5	0.3	0.5		0.2
4α23,24-Trimethyl Δ0	0.6	0.4	0.7	0.4	1.9	1.0	1.7	2.2	3.1	2.3	1.4	2.2	3.0	3.5	1.3	2.6	1.1	0.9	1.2	1.7	0.8	3.5	0.6	4.5	3.4		0.3		0.6	0.4	0.2	1.1		0.4
4α,24-Dimethyl Δ0	n.d.	n.d.	n.d.	0.4	1.5	0.9	1.7	0.5	1.6	0.6	1.0	2.4	2.7	0.8	1.9	n.d.	n.d.	n.d.	n.d.	n.d.	n.d.	n.d.	n.d.	0.5	n.d.		n.d.		0.1	0.1	n.d.	n.d.		n.d.
C30 alkane 1,15 diol (+1,14 + 1,13)	0.4	0.8	0.6	1.3	3.3	3.8	7.9	4.5	7.7	4.1	2.0	2.6	4.4	7.5	2.0	4.1	0.8	0.6	1.2	1.4	1.5	3.6	5.2	5.1	7.1		0.6		0.5	0.6	0.5	0.7		0.3
C30 kétol	1.3	0.7	1.0	1.2	3.3	4.4	6.7	4.0	5.8	3.5	1.9	2.4	3.2	9.3	1.7	3.5	0.8	1.0	1.4	1.2	1.4	4.2	4.5	4.7	5.9		0.3		0.3	0.7	0.4	1.1		2.2
Mid-chain alkanol	0.2	0.1	0.1	0.3	1.0	0.8	1.1	0.4	0.6	0.5	0.2	0.6	0.5	2.1	0.3	0.9	0.1	0.2	0.1	0.4	0.2	0.7	n.d.	n.d.	0.7		n.d.		0.6	n.d.	n.d.	0.2		0.1

Table 5. Comparison of the abundance of C29 sterols, of higher plant n-alkanes and of higher plant n-alkanols in aerosols and in sinking particles collected during DYNAPROC 2. The left side of the table comprise concentrations, the right side of the table comprise abundance of biomarkers normalized to the abundance of long-chain n-alkanes. Minima and maxima are given on top lines; average and standard deviation, when available, are given in brackets on the second lines. [a] Sum of n-alkanes, but they are mostly long-chain odd alkanes. [b] Sum of n-alkanols, but they are mostly long-chain even alkanols.

Location	long-chain n-alkanes	long-chain n-alkanols	Δ5	24EtΔ5	24EtΔ5,22E	long-chain n-alkanols	Δ5	24EtΔ5	24EtΔ5,22E	References
Marine aerosols			ng m^{-3}			normalized to long-chain n-alkanes, relative unit				
Azores	0.3–6.18[a] (1.11)	0.75–18.6[b] (3.47)	0.002–0.209	0.01–0.139	(3.1)	2.5–3.0	0.01–0.03	0.01–0.03		Alves et al. (2007)
North Pacific	0.11–14.1[a] (1.8)	0.18–19.7 (2.2)	nd–0.89 (0.053)	nd–0.30 (0.066)		1.4–1.6 (1.2)	nd–0.06 (0.03)	nd–0.03 (0.04)		Kawamura et al. (2003)
Korea	2.31–14.0 (7.94)	3.38–53.2 (26.28)	nd–2.19 (0.38)	nd–11.4 (2.28)	nd–13.6 (2.66)	1–4 (3.3)	nd–0.16 (0.05)	nd–0.81 (0.29)	nd–0.97 (0.34)	Wang et al. (2009)
Sinking particles NW Mediterranean	0.16–3.2 (1.2±0.8)	nd–1.2 (0.3±0.3)	μg (mg OC)$^{-1}$ 0.68–18.6 (6.1±3.8)	1.73–9.3 (3.6±1.5)	0.83–4.7 (2.2±1.0)	normalized to long-chain n-alkanes, relative unit nd–156 (47±31)	0.11–62 (10±11)	1.7–22 (5.6±3.5)	0.8–7.4 (3.4±1.7)	This work

L. Méjanelle and J. Dachs

Title Page

Abstract | Introduction

Conclusions | References

Tables | Figures

◀◀ | ▶▶

◀ | ▶

Back | Close

Full Screen / Esc

Printer-friendly Version

Interactive Discussion

Table 6. Comparison of the biomarker fluxes measured in DYNAPROC2 high frequency sediment trap experiment and selected literature. [a] Flux of the sum of C37, C38 and C39 alkenones. [b] Flux of $4\alpha,23,23$-trimethylcholest-22-en-3β-ol (dinosterol). [c] Flux of the summed C_{37} and C_{38} alkenones. [d] Flux of C37:2 methyl alkanone. [e] Flux of 24-methylcholesta-5,24(28)-dien-3β-ol.

Location	Depth	Resolved hydrocarbons	C_{37} alkenones	C_{30} alkane diol	Sum sterols	Reference
New Guinea Coast	300–1460 m	2.6–46.5			13–602	Burns et al. (2004)
Australian Shelf	300–1430 m	29.7–36.8			13–602	Burns et al. (2004)
NW Autralian Shelf	200–600 m	30–37			6–16.5	Burns et al. (2003)
Eastern North Pacific						
High productivity site	740–4750 m	2.7–5.6				Matsueda and Handa (1986)
Low productivity site	741–4750 m	0.37–0.82				Matsueda and Handa (1986)
Arabian Sea	2220 m	0.22–2.64	0.87–40.8[a]		nd–7.92[b]	Prahl et al. (2000)
Antarctic HLNC zone	200 m	0.1–8.3	0–77.2[c]		68–661	Ternois et al. (1998)
SW Pacific Ocean	300–1000 m		0.05–95		Oct 1998	Sikes et al. (2005)
N Pacific	140 m				ca. 50–220	Wakeham and Lee (1989)
N Pacific	100 m				ca. 1200	
N Pacific	505 m–3380 m		0.11–1.97[d]	2.6–9.29	3.7–16.4[e]	Wakeham et al. (2002)
N Pacific	1235–3815				15–110	Grimalt et al. (1990)
NAtlantic	2865–4730				19–78	Grimalt et al. (1990)
NE Atlantic	3700 m		nd–5			Rosell-Melé et al. (2000)
Mediterranea, Alboran Sea	100 m		12.8–31.7		288–817	Tolosa et al. (2005)
	300 m		2.60–15.7		95.5–294	
Mediterranan, DYFAMED site	200 m	2.1–34.7				Marty et al. (1994)
Mediterranan, DYFAMED site	200 m		0–9			Ternois et al. (1997)
Mediterranan, DYFAMED site	200 m	1.4–29.7	0–14.2	0.3–9.3	31–377	This work

Table 7. Pearson matrix of correlation between fluxes of selected of biomarkers; Pearson Corr. coeff.: Pearson correlation coefficient. Sigma expresses the probablity of non correlation ($p = 1 - \mathrm{sigma}$).

		C37 alkenones	Δ5,22	Δ5	24MeΔ5,22	24 Me Δ5,24(28)	cholest-4-en-3-one	24 Et Δ5	4α,23,24 triMe Δ22	C30 alkyl diol	Sum C22–C26-OH	Alcene C37:3	Sum odd HNA C≥25	Organic Carbon
C37 alkenones	Pearson Corr. coeff.	1	.824[b]	.685[b]	.891[b]	.593[b]	.864[b]	.906[b]	.910[b]	.881[b]	.683[b]	.848[b]	.761[b]	.796[b]
	Sigma (bilateral)		.000	.000	.000	.000	.000	.000	.000	.000	.000	.000	.000	.000
	N	31	31	31	31	31	17	31	31	31	31	26	28	31
Δ5,22	Pearson Corr. coeff.	.824[b]	1	.647[b]	.887[b]	.627[b]	.838[b]	.878[b]	.853[b]	.808[b]	.643[b]	.823[b]	.831[b]	.877[b]
	Sigma (bilateral)	.000		.000	.000	.000	.000	.000	.000	.000	.000	.000	.000	.000
	N	31	31	31	31	31	17	31	31	31	31	26	28	31
Δ5	Pearson Corr. coeff.	.685[b]	.647[b]	1	.627[b]	.478[b]	.811[b]	.656[b]	.633[b]	.683[b]	.413[a]	.666[b]	.597[b]	.626[b]
	Sigma (bilateral)	.000	.000		.000	.006	.000	.000	.000	.000	.021	.000	.001	.000
	N	31	31	31	31	31	17	31	31	31	31	26	28	31
24MeΔ5,22	Pearson Corr. coeff.	.891[b]	.887[b]	.627[b]	1	.713[b]	.968[b]	.993[b]	.981[b]	.865[b]	.796[b]	.905[b]	.910[b]	.828[b]
	Sigma (bilateral)	.000	.000	.000		.000	.000	.000	.000	.000	.000	.000	.000	.000
	N	31	31	31	31	31	17	31	31	31	31	26	28	31
24Me Δ5,24(28)	Pearson Corr. coeff.	.593[b]	.627[b]	.478[b]	.713[b]	1	.845[b]	.712[b]	.752[b]	.669[b]	.411[a]	.593[b]	.658[b]	.686[b]
	Sigma (bilateral)	.000	.000	.006	.000		.000	.000	.000	.000	.021	.001	.000	.000
	N	31	31	31	31	31	17	31	31	31	31	26	28	31
cholest-4-en-3-one	Pearson Corr. coeff.	.864[b]	.838[b]	.811[b]	.968[b]	.845[b]	1	.975[b]	.966[b]	.882[b]	.822[b]	.870[b]	.915[b]	.821[b]
	Sigma (bilateral)	.000	.000	.000	.000	.000		.000	.000	.000	.000	.000	.000	.000
	N	17	17	17	17	17	17	17	17	17	17	13	15	17
24 Et Δ5	Pearson Corr. coeff.	.906[b]	.878[b]	.656[b]	.993[b]	.712[b]	.975[b]	1	.992[b]	.899[b]	.799[b]	.916[b]	.908[b]	.835[b]
	Sigma (bilateral)	.000	.000	.000	.000	.000	.000		.000	.000	.000	.000	.000	.000
	N	31	31	31	31	31	17	31	31	31	31	26	28	31
4α,23,24 triMe Δ22	Pearson Corr. coeff.	.910[b]	.853[b]	.633[b]	.981[b]	.752[b]	.966[b]	.992[b]	1	.918[b]	.758[b]	.913[b]	.887[b]	.845[b]
	Sigma (bilateral)	.000	.000	.000	.000	.000	.000	.000		.000	.000	.000	.000	.000
	N	31	31	31	31	31	17	31	31	31	31	26	28	31
C30 alkyl diol	Pearson Corr. coeff.	.881[b]	.808[b]	.683[b]	.865[b]	.669[b]	.882[b]	.899[b]	.918[b]	1	.573[b]	.834[b]	.769[b]	.881[b]
	Sigma (bilateral)	.000	.000	.000	.000	.000	.000	.000	.000		.001	.000	.000	.000
	N	31	31	31	31	31	17	31	31	31	31	26	28	31
Sum C22-C26-OH	Pearson Corr. coeff.	.683[b]	.643[b]	.413[a]	.796[b]	.411[a]	.822[b]	.799[b]	.758[b]	.573[b]	1	.762[b]	.813[b]	.485[b]
	Sigma (bilateral)	.000	.000	.021	.000	.021	.000	.000	.000	.001		.000	.000	.006
	N	31	31	31	31	31	17	31	31	31	31	26	28	31
Alcene C37:3	Pearson Corr. coeff.	.848[b]	.823[b]	.666[b]	.905[b]	.593[b]	.870[b]	.916[b]	.913[b]	.834[b]	.762[b]	1	.851[b]	.760[b]
	Sigma (bilateral)	.000	.000	.000	.000	.001	.000	.000	.000	.000	.000		.000	.000
	N	26	26	26	26	26	13	26	26	26	26	26	26	26
Sum odd HNA C≥25	Pearson Corr. coeff.	.761[b]	.831[b]	.597[b]	.910[b]	.658[b]	.915[b]	.908[b]	.887[b]	.769[b]	.813[b]	.851[b]	1	.708[b]
	Sigma (bilateral)	.000	.000	.001	.000	.000	.000	.000	.000	.000	.000	.000		.000
	N	28	28	28	28	28	15	28	28	28	28	26	28	28
Organic Carbon	Pearson Corr. coeff.	.796[b]	.877[b]	.626[b]	.828[b]	.686[b]	.821[b]	.835[b]	.845[b]	.881[b]	.485[b]	.760[b]	.708[b]	1
	Sigma (bilateral)	.000	.000	.000	.000	.000	.000	.000	.000	.000	.006	.000	.000	
	N	31	31	31	31	31	17	31	31	31	31	26	28	31

[b] The correlation is significant at the 0,01 level (2-paired).
[a] The correlation is significant at the 0,05 level (2-paired).

Title Page

Abstract | Introduction

Conclusions | References

Tables | Figures

◀ | ▶

◀ | ▶

Back | Close

Full Screen / Esc

Printer-friendly Version

Interactive Discussion
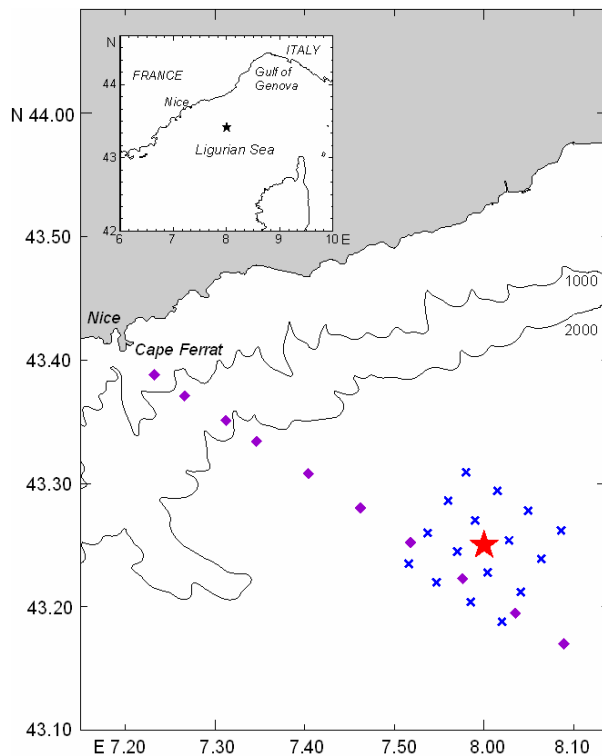
Fig. 1. Location of sampling site (red star) and grid of stations (blue crosses) of the DY-NAPROC 2 cruise.
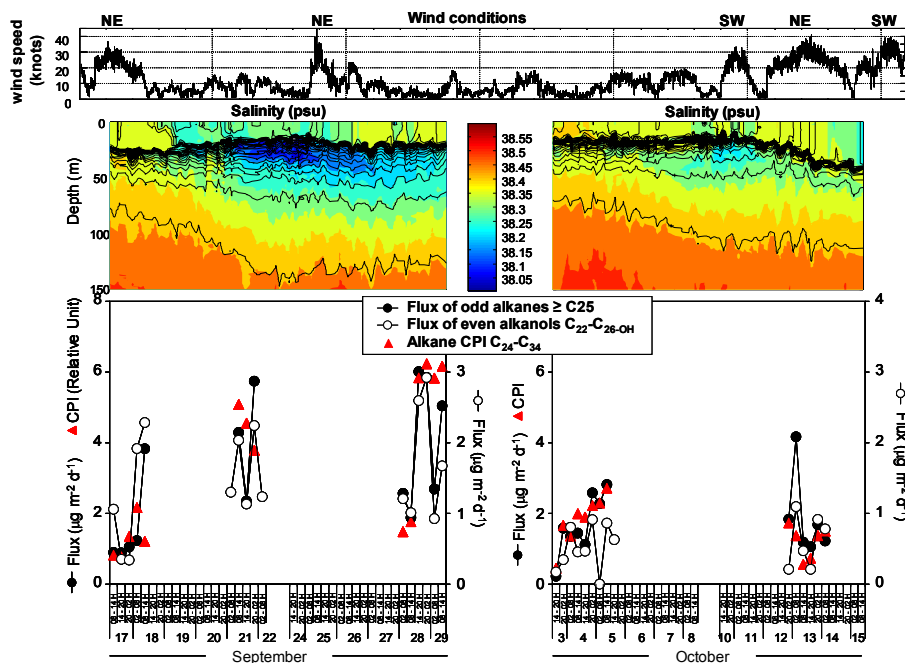
Fig. 2. Upper panel: Time series wind conditions during DYNAPROC 2. Wind speed is plotted in knots and wind direction is given above the panel. Middle panel: Time-series salinity profiles. The blue color shows the intrusions of low salinity waters at the study site. Lower pannel: Fluxes of higher plant biomarkers: odd *n*-alkanes having 25 C atoms and more and even *n*-alkanols having 22, 24 and 26 C atoms. Red triangles indicate the Carbon Preference Index of *n*–alkanes in the C range C_{24} to C_{34}. Grey filling indicate night-time collection of particles.

Fig. 3. Fluxes of organic carbon and fluxes of sterols, alkenones and hydrocarbons measured at 200 m during DYNAPROC 2. Organic carbon data are from Marty et al. (2009).

L. Méjanelle and J. Dachs
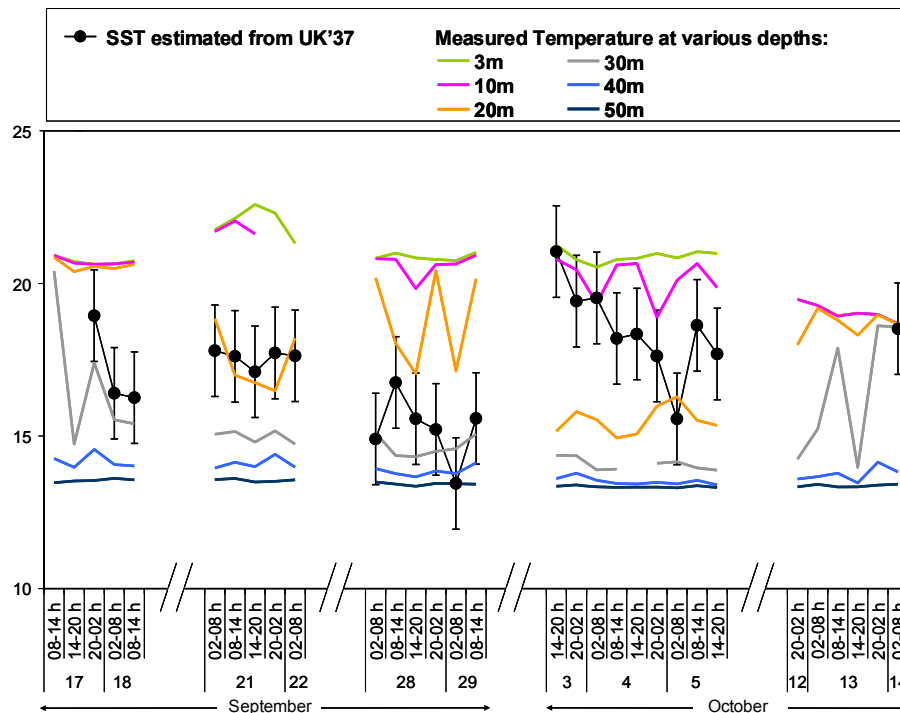
Fig. 4. Comparison of SST reconstructed using the alkenone unsaturation index UK$'_{37}$ and hydrocast temperatures at various depths. The x-axis represents time of particles collection and is discontinous.
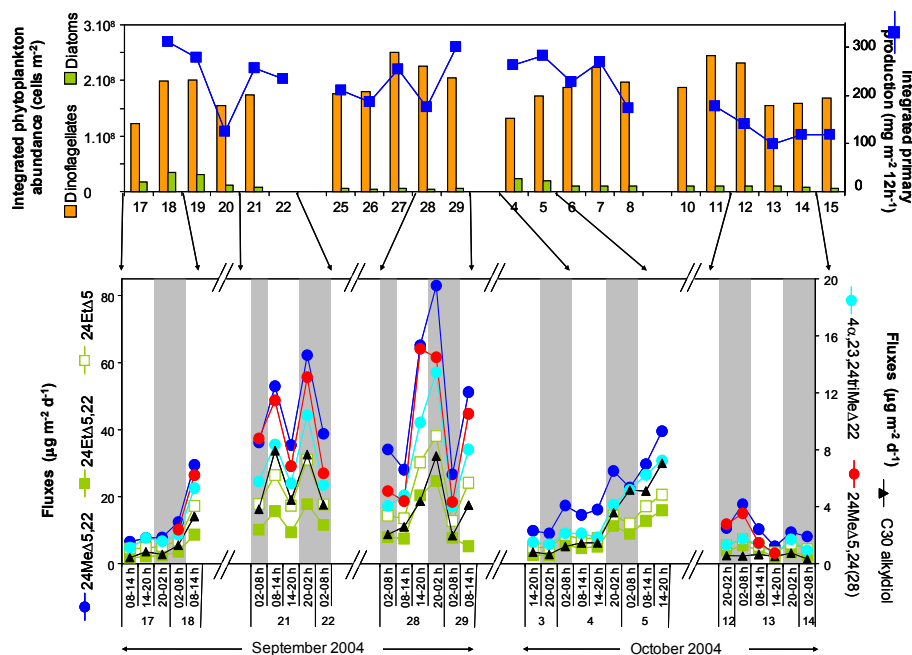
Fig. 5. Water column primary production and biomarker export during DYNAPROC 2. Upper pannel: Time-series primary production integrated over the 60 upper meters of the water column (data from Marty et al., 2008), and abundance of microphytoplankton integrated over the 60 upper meters of the water column (data from Lasternas et al., 2008). Lower panel: Time series fluxes of selected phytoplanktonic biomarkers. 24MeΔ5,22: 24-methylcholesta-5,22E-dien-3β-ol; 24EtΔ5,22: 24-ethylcholesta-5,22E-dien-3β-ol; 24EtΔ5: 24-ethylcholesta-5-en-3β-ol; 4α,23,24triMeΔ22: α,23,24-trimethylcholesta-22E-en-3β-ol; 24MeD5,24(28): 24-methylcholesta-5,24(28)-dien-3β-ol. The x-axis on the lower panel represents time of collection of particles and is discontinuous, arrows between both panels indicate time correspondance. Grey filling indicate night-time collection of particles.

Title Page

Abstract | Introduction

Conclusions | References

Tables | Figures

◄◄ | ►►

◄ | ►

Back | Close

Full Screen / Esc

Printer-friendly Version

Interactive Discussion
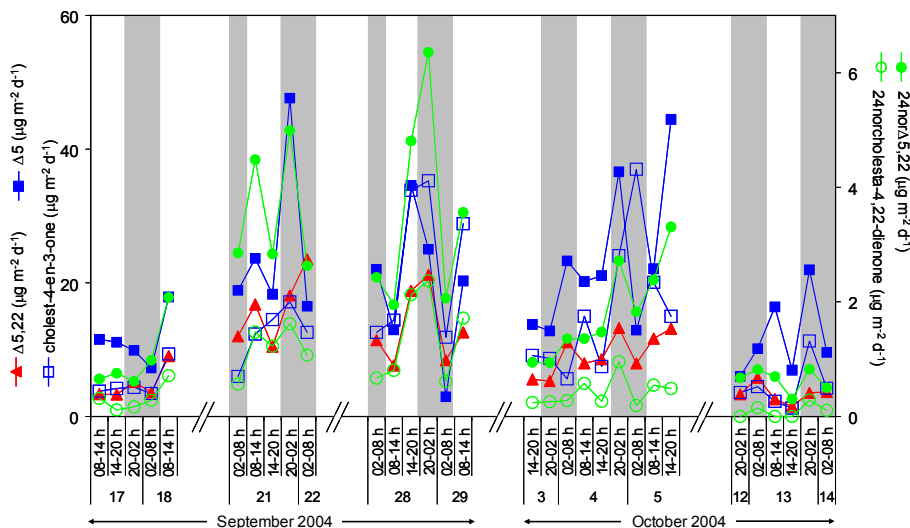
Fig. 6. Fluxes of sterols in part contributed by zooplankton: Δ5: cholest-5-en-3β-ol: Δ5,22:cholesta-5,22E-dien-3β-ol. 24-norΔ5,22: flux of 24-nor-cholesta-5,22E-dien-3β-ol. Fluxes of steroid ketones: cholest-4-en-3-one, oxidation product of cholest-5-en-3β-ol, and 24-nor-cholesta-4,22E-dienone, oxidation product of 24-*nor*-cholesta-5,22E-dien-3β-ol. The x-axis represents the time of collection of drifting sediment traps and is discontinuous. Grey filling indicate night-time collection of particles.